





Received February 11, 2020, accepted February 23, 2020, date of publication March 5, 2020, date of current version March 30, 2020.

Digital Object Identifier 10.1109/ACCESS.2020.2978531

# Wireless AI in Smart Car: How Smart a Car Can Be?

QINYI XU<sup>1</sup>, BEIBEI WANG<sup>1</sup><sup>2</sup>, (Senior Member, IEEE), FENG ZHANG<sup>1</sup><sup>2</sup>, (Member, IEEE), DEEPIKA SAI REGANI<sup>1</sup><sup>3</sup>, FENGYU WANG<sup>3</sup>, AND K. J. RAY LIU<sup>1</sup><sup>3</sup>, (Fellow, IEEE)

<sup>1</sup>Facebook Inc., Menlo Park, CA 94025, USA

<sup>2</sup>Origin Wireless, Inc., Greenbelt, MD 20770, USA

<sup>3</sup>Electrical and Computer Engineering Department, University of Maryland at College Park, College Park, MA 20742, USA

Corresponding author: Beibei Wang (beibei.bbwang@gmail.com)

**ABSTRACT** In the era of the Internet of Things (IoT), billions of smart devices connect, interact, and exchange data with each other. As “things” get connected together, intelligent systems and technologies have been developed to exploit the rich information in the collected data, perceive what is happening in the surroundings, and finally take actions to maximize their own utility. Thanks to the ubiquitous wireless signals and the prevalence of wireless devices, wireless sensing becomes more popular among the various approaches that have been adopted in the IoT to measure the surrounding environment. Because human activities interact with wireless signals and introduce distinct patterns to the propagation, analyzing how wireless channel state information (CSI) responds to human activities enables many IoT applications. Recently, radio analytics has been proposed as a promising technique that exploits multipath as virtual antennas, extracts various features from wireless signals, and reveals rich environmental information. As automobiles continue to play an important role nowadays, manufacturers have been seeking emerging techniques for IoT applications that support drivers and enhance safety. The interior of an automobile can be viewed as a special indoor environment where most of the multipaths are restricted inside by the metal exterior. In this article, we introduce the concept of wireless artificial intelligence (AI) and demonstrate its concept in a smart car scenario where information about drivers and passengers is collected by commercial Wi-Fi devices deployed in the car. The proposed wireless AI system is capable of identifying authorized drivers based on radio biometric information. Vital signals of human introduce periodic patterns to the wireless CSI. By extracting the vital sign from wireless signals, the proposed wireless AI system can monitor the driver’s state, count number of people in the car, and detect a child left in an unattended car.

**INDEX TERMS** Child presence detection, in-car monitoring, smart car, wireless artificial intelligent.


## I. INTRODUCTION

The Internet of Things (IoT) refers to the smart devices and sensors that are deployed in the environment and connected so that they can gather, share and integrate information. Many emerging IoT technologies and systems have been designed to facilitate people understanding human activities in surrounding environments. It has been envisioned that wireless sensing will become a prominent solution to the IoT applications due to the proliferation of wireless radio devices, ubiquitous wireless signals, and the rich information introduced into the wireless signals by human activities.

The feasibility of wireless sensing comes from the fact that environmental information is recorded in wireless sig-

nals. Nature provides numerous degrees of freedom that is delivered through wireless multipath propagation. Multipath propagation is the phenomenon that the received signal at the receiver side is a collection of signals traveling from the same source but through different paths. Due to the large number of multipaths in a rich scattering indoor environment, information with a large degree of freedom can be captured by wireless signals. However, the performance of wireless sensing highly relies on the information richness we can decipher from the received wireless signal and it is determined by the transmission bandwidth. Nowadays, with advanced wireless communication technologies, more bandwidths become available and richer information can be revealed from wireless signals.

As originated from the time reversal (TR) technique, radio analytics has been proposed as the technique that exploits

The associate editor coordinating the review of this manuscript and approving it for publication was Muhammad Maaz Rehan .

the wireless signal, or more specifically the wireless channel state information (CSI), extracts various features and then interprets the environmental information around us [1]. TR technique treats each indoor multipath as a distributed virtual antenna and generates a high-resolution spatial-temporal focusing effect, also known as the TR resonance effect [2]–[4]. The TR resonance effect is a result of the resonance of the electromagnetic (EM) field in response to the environment, a.k.a. the interaction between the wireless signal and its multipath propagation [5]. When the indoor environment changes, the multipath propagation varies accordingly and it results in a decrease in the TR resonance strength. Along with the TR technique, various radio analytic techniques have been developed to analyze radio signals, decipher the embedded environmental information, and support different IoT applications.

On one hand, human activities or moving objects introduce dynamics to the propagation of wireless signals. By deploying wireless sensors, extracting and analyzing various features implanted in wireless signals, one can infer macro changes in the indoor environment, such as indoor events detection [6]–[9], human activities recognition [10]–[17], indoor positioning [18]–[27], gait recognition [28]–[30] and tracking [31]–[34]. Moreover, one can also detect micro changes including hand gestures [35], [36] and vital signs [38]–[41] without requiring any wearable devices. Those IoT applications can be an ideal solution to home and office security systems, human activity recognition systems and well-being monitoring systems. On the other hand, each human body will introduce unique perturbations to the wireless signals, through absorbing, reflecting and scattering wireless signals [42], [43]. The static wireless propagation pattern interacted with a human body is defined as human radio biometrics, which is determined by individual biological characteristics. With the help of radio analytics, indoor human recognition now can be achieved through a non-vision based technique through radio biometrics [44].

Due to its on-demand transportation, mobility, independence, convenience, and comfortableness, automobiles have become a daily commodity with surging demand and prevalence. According to the report [45], [46], the number of worldwide automobiles on-the-road has reached 1.2 billion by 2017 and the U.S. vehicle ownership per household achieved 1.97 in 2016. In the past decade, automobile manufacturers and researchers have been working on innovative solutions that leverage emerging sensor technology to support the driver and enhance the safety, e.g., driver monitoring system to detect distraction and fatigue [47]–[51].

In contrast to most of the existing in-car techniques which require contact sensors and cameras [52], radio analytics that relies only on wireless signals is a promising solution to smart car monitoring. Nowadays, many car manufacturers are adding built-in Wi-Fi equipment to their new vehicles and internet providers are collaborating with them to provide cheap and fast Wi-Fi service. Secondly, superior to traditional sensors, Wi-Fi not only acts as an in-car sensor but also serves to connect passengers and drivers to the internet. On the other

hand, what makes Wi-Fi an ideal solution for in-car sensing is that it can work under the circumstances of obstructions thanks to the multipath propagation, which is impossible for traditional sensors and cameras. The interior of a car can indeed be viewed as a special indoor environment where most of the multipaths are confined inside the car because of the metal exterior. By deploying wireless radio devices in a car, radio analytics can enable many IoT applications specialized for automobile uses that have been envisioned for a long time but not been accomplished yet.

In this article, we will present the concept of wireless artificial intelligent (AI) which performs radio analytics, perceives the environment, and then takes optimal actions for different applications [53]. We demonstrate the capability of wireless AI through a smart car scenario. We first provide an overview of fundamental concepts of radio analytics and the multipath harvesting. Then we define the smart car scenario and propose to use a single pair of commercial Wi-Fi devices to achieve 4 different IoT applications, including driver authentication, vital sign monitoring, passenger counting, and unattended child detection for parked cars.

To begin with, we first introduce the wireless AI driver authentication system that only allows an authorized driver to operate the car, guaranteeing the security and safety of automobiles. With a pair of commercial Wi-Fi devices deployed in the car, the biological information of the driver will be recorded by wireless signals. The proposed wireless AI smart car system extracts the radio biometric information of the driver and achieves accurate driver recognition and authentication. We further demonstrate how the proposed wireless AI system captures vital signs from the wireless signals to assist driver state monitoring, passenger counting and unattended child detection. By analyzing the periodic pattern implanted in the wireless signal, the proposed wireless AI system can monitor the real-time breathing rate of the driver, which serves as an important indicator for health and fatigue in driver state monitoring. Moreover, by performing further analysis of the vital features recorded in the CSI, the proposed wireless AI system can count the number of people in the car. Inspired by the in-car vital monitoring, the proposed wireless AI system is also capable of detecting whether a child is left unattended in the car, which is extremely dangerous and even can be fatal [54]. Finally, we will survey and discuss recent related works.

## II. CHALLENGES AND CONTRIBUTIONS

*Challenge 1:* Traditional dedicated sensors in the car require line-of-sight between the sensors and the objects being monitored.

This work presented a novel concept of wireless artificial intelligence (AI) that perceives the propagation environment with a pair of Wi-Fi devices through radio analytics and demonstrated the concept with a smart car scenario. Thanks to the multipath propagation of wireless signals, the proposed Wi-Fi based in-car sensing system can perceive the environment even when there are obstructions.

**Challenge 2:** Previous wireless-sensing-based human identification systems are susceptible to changing CSI because that the indoor/in-car environment always changes over time.

This work proposed an in-car Wi-Fi-based driver authentication system which addresses the challenges of varying environment by means of machine learning (ML). The proposed ML based system can generalize consistent radio biometric information from collected CSI samples captured under changing environments in a car.

**Challenge 3:** Current in-car driver monitoring systems require either cameras or contact sensors to monitor the biological signals of a driver, which may be distracting or have privacy concerns.

This work proposed an in-car vital sign monitoring system that estimates the breathing frequency of the driver by extracting the periodical pattern from the captured time series of CSI. Because of the multipath propagation of wireless signals, the proposed system can be installed away from the driver and the passengers to ensure privacy and safety.

**Challenge 4:** In current vehicles, the number of passengers inside a car is estimated through pressure sensors installed under each seat and the accuracy is low because the pressure sensor can be triggered by heavy objects like luggage while it may fail to respond to a child of lightweight.

This work proposed a novel method of people counting by identifying and counting distinct human breathing rate traces in the environment, even without line-of-sight between the monitored individuals and the Wi-Fi devices. A dynamic programming (DP) based trace tracking algorithm was designed that extracts and tracks breathing signals of different individuals in the car from the time series of CSI captured by a pair of commercial Wi-Fi devices.

**Challenge 5:** Existing child presence detection (CPD) systems may fail to detect the presence of a child when the weight of the child is too light for a pressure sensor or the child is blocked from the line-of-sight of a camera.

This work proposed a novel in-car CPD method that utilizes Wi-Fi multipath propagation to detect the dynamics introduced by child movement or breathing and has no blind zone.

### III. RADIO ANALYTICS: FUNDAMENTALS

Wireless sensing takes advantage of a large number of degrees of freedom provided by nature by means of radio multipath propagation. When a signal encounters a scatterer in the environment, an attenuated copy of the original signal is generated and will travel through a new path. Because of the existence of the scatterers in the environment, the transmit signal emitted from the transmitter (TX) arrives at the receiver (RX) through different propagation paths and the channel between each TX-RX antenna becomes a multipath channel. This is known as multipath propagation. An illustration of a multipath channel is depicted in FIGURE 1. The red line represents the line-of-sight (LOS) path from the TX to the RX, while the blue arrows plot the reflected/scattered

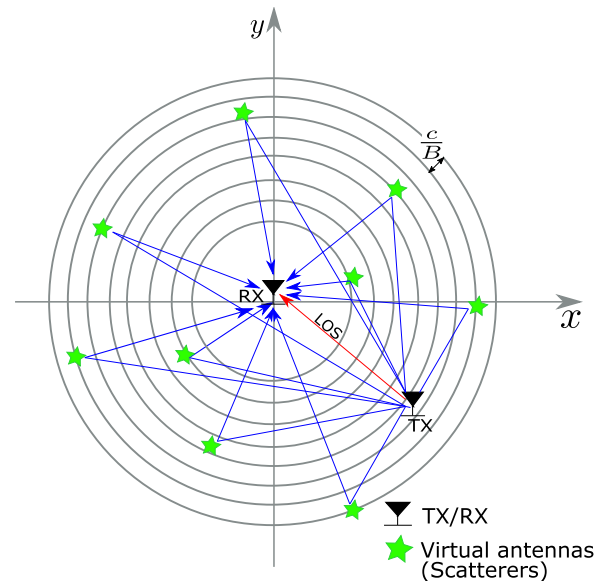


FIGURE 1. Illustration of virtual antennas [55].

path by scatterers in the environment. All the paths form a multipath propagation channel between the TX and the RX [55].

Because an attenuated copy of the original signal is generated and transmitted through a different path when the transmit signal gets reflected or scattered by a scatterer, each multipath acts as a virtual antenna and/or sensor in the environment that collects and transmits the replica data from a different spatial location, providing an extra degree of freedom. The channel characteristics between the virtual antenna and the real antenna are determined by the radio paths both between the TX and the scatterer and between the scatterer and the RX. Daily activities involve motion and human body movements which can be viewed as groups of moving scatterers/virtual antennas in the environment. As the radio signal propagates back and forth between the scatterers, the characteristics of the virtual antennas are recorded in the multipath CSI, and so does the information about indoor activities. The performance of wireless sensing depends greatly on how rich the CSI can be. The transmission bandwidth determines the spatial resolution of the CSI to reveal different multipath components.

Through channel sounding, real-time CSI can be estimated that records the information of all scatterers in the environment encountered during the radio propagation. In an environment with  $K_{max}$  independent multipath components existing between the TX and the RX, the multipath channel  $h(t)$  is defined as collections of different radio propagation paths,

$$h(t) = \sum_{k=1}^{K_{max}} \alpha_k \delta(t - \tau_k), \quad (1)$$

where  $\alpha_k$  is the multipath coefficients of the  $k$ -th independent multipath component and  $\tau_k$  is the time delay associated

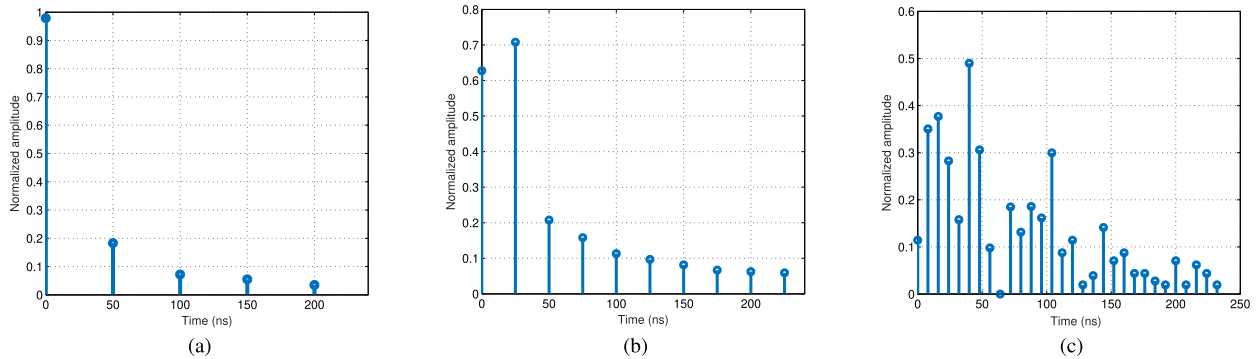


**FIGURE 2. Multipath channel vs bandwidth. (a) Measured channel under 20 MHz bandwidth (LTE standard). (b) Measured channel under 40 MHz bandwidth (the IEEE 802.11n standard). (c) Measured channel under 125 MHz bandwidth (entire ISM 5G band) [55].**

with  $\alpha_k$ . The function  $\delta(\cdot)$  is the delta function. Note that, the delay spread of the channel is  $\tau = \max_k \tau_k$ .

However, due to the limited transmission bandwidth  $B$ , the estimated discrete-time channel  $\mathbf{h}_T$  at the receiver side is a sampled version of  $h(t)$ , i.e.,

$$h_T[l] = \int_{\frac{l-1}{B}}^{\frac{l}{B}} P\left(\frac{l}{B} - t\right)h(t)dt, \quad l = 0, 2, \dots, L - 1, \quad (2)$$

where  $P(\cdot)$  is the window function with length  $1/B$ . Because signals with time-of-flight (ToF) difference equal to or larger than  $1/B$  can be separated under a bandwidth  $B$ , a larger bandwidth enables a higher sampling rate to sample analog signals received from different paths and resolve more multipath components.

Examples of multipath channels captured under the aforementioned bandwidths at the same location in a rich-scattering environment are plotted and compared in FIGURE 2, demonstrating the relationship between bandwidth and multipath resolution. As projected in 5G, high carrier frequencies with larger bandwidths will be adopted in future wireless communication systems [56], which makes the multipath channel with a good spatial resolution feasible. With more and more bandwidth readily available for the next generation of wireless sensing, many more smart applications/services will come true, because richer information becomes available with a wider bandwidth.

With rich information embedded in the radio signals, now the challenge is how to utilize it to help people perceive and understand surrounding activities. Various techniques have been proposed to harvest information from the multipath CSI. By treating each multipath components as a virtual antenna that transmits probing signal coherently (a.k.a., TR transmission process [57]), TR technique generates a high-resolution spatial-temporal resonance, which can be viewed as the result of the resonance of EM field in response to the environment [5]. As long as a change occurs on either the device or any scatterer in the environment, the corresponding multipath channel between the TX and the RX changes accordingly. Consequently, the TR spatial-temporal resonance changes,

which in return indicates the changes in the propagation environment.

Inspired by the fundamental physical principle of TR, *Radio analytics* has been proposed as an emerging technology that infers the propagation environment and extends the human sense over the world [1]. By fully exploiting the rich multipath CSI, various types of radio analytics based on the wireless channel state information has been developed to enable many cutting-edge IoT applications indoors, including positioning and tracking, vital monitoring, indoor event detection and activity recognition, and human identification, as we will discuss in Section IX.

#### IV. SMART CAR MONITORING

As the most widely accepted and popular method of transportation, automobiles have become a necessity and essential part of people’s everyday life and profoundly changed the way people live all over the world. In spite of its benefits in on-demand mobility, convenience, and comfortableness, the prevalence of automobiles has also brought up risks including road safety and environmental pollution. Over the decades, as automobiles brought various influences to every aspect of the society, innovative technologies have been introduced to automobile for driving assistance and safety enhancement.

##### A. DRIVER STATE MONITORING

Road safety is always the top concern for automobiles. Statistics show that a lack of driver’s attention during driving due to sleepiness, distraction, drowsiness, and stress is the major factor in vehicle crashed accidents. According to [58], 94% of crashes in the United States between 2005 and 2007 were attributed to drivers, such as recognition errors due to inattention, decision errors, performance errors, and non-performance errors like sleep. Research and industry have been developing in-car driver monitoring systems to avoid driver risk factors and bad driving operation in advance [52], [59], [60]. Current technologies implement in-car driver monitoring by means of cameras [49], [61], [62] and physiological sensors for electroencephalogram (EEG)



or/and electrocardiogram (ECG) signals [52], [63]–[65]. Recently, a Wi-Fi-based driver distraction monitoring system was proposed by Raja *et al.* to detect unusual head turns and arm movements by leveraging features in the CSI [66].

### B. AUTHORIZED DRIVER IDENTIFICATION

Another important factor that impacts automobile safety is that automobiles nowadays can be operated by anyone with access to the car key, and driving by an unauthorized driver can lead to an increased risk of a crash. Automobile driving is an activity where the driver has to be able to simultaneously watch for surroundings, control and operate the vehicle, manage unexpected events, and make decisions. For example, younger and particularly novice drivers, who have little knowledge of driving or have no driver's license, lack sufficient skills to recognize or anticipate road hazards and often tend to speed. It is important that the future smart car can leverage biometric information of each individual and perform identity recognition to allow driving by authorized drivers only.

### C. PASSENGER MONITORING

While most advanced technologies for the smart car focused on driver state monitoring, limited research has been conducted for in car passenger monitoring. For most of the automobiles today, pressure sensors are installed under a seat to detect seat occupancy and enable associated air bags. However, pressure sensors tend to fail in distinguishing between a human body and an item with a similar weight. In the era of IoT, many techniques have been developed with which various sensors can sense the activities in an environment, including human vital signs. By analyzing the vital signs, it is possible for a smart car to monitor the well-being of passengers and even count how many people sitting inside.

### D. CHILD PRESENCE DETECTION (CPD)

Children left inside an unattended car can be extremely dangerous. According to the report in [54], an average of 38 children die of heatstroke inside hot vehicles each year, and there is a total of 792 Pediatric Vehicular Heatstroke (PVH) deaths that have been documented in the United States for the period from 1998 to 2018. Among those, 53.9% of the PVH deaths are due to that parents left their child in the car and 26.4% are due to the child having gained access to the car without letting the parents know. However, because most of the kids are put inside a car seat on the back seat and the weight is light, current pressure sensors and cameras fail to detect their presence. Hence, it is critical and urgent to develop in-car monitoring systems that can detect promptly when a child is left inside a locked car even with obstruction and thus avoid such a tragedy.

Although researchers and manufacturers focus on developing techniques to address the aforementioned problems, they often require various sensors dedicated to each application. Unlike dedicated sensors which can only be used for sensing, Wi-Fi is superior in that it can serve as both in-car sensors



FIGURE 3. Illustration of in-car multipath propagation.

and in-car connection devices to connect passengers and drivers to the internet while traveling. A car is a special case of rich scattering indoor environments where radio waves bounce back and forth by the metal exterior, as illustrated in FIGURE 3. First, the interior of a car is like a metal box with most of the multipaths only traveling inside, because radio waves cannot penetrate metal. Second, the movement of the car will not affect the propagation inside a lot, since the transmission, engine, wheels are all located outside the main cargo which is concealed by metal. Moreover, as we tested and verified in the experiment [67], the outside environment changes will not affect the multipath environment inside the car. Hence, the interior of a car can be viewed as an indoor environment with rich multipath propagation and its moving status will not impact a lot on RF sensing.

Given the plentiful multipaths inside a car, radio analytics provides a feasible and promising solution to smart car applications. Thanks to the multipath propagation, activity and biological information of people inside a car can be sensed and captured, which supports wireless sensing applications on identity recognition and vital monitoring. Anomaly detection can also be realized for a parked car by detecting dynamic changes in the CSI. Because most of the multipaths are restricted inside the car, outside activities can hardly introduce false alarms. In this article, we propose a wireless AI system for smart car such that with a single pair of commercial Wi-Fi devices deployed in the car, the in-car environmental information can be extracted from the wireless signals that reveals the enriched information of driver identity, driver vital state, passenger well-being, and the presence of a left child in a parked car. In the following sections, we will discuss the details of the proposed wireless AI smart car system and demonstrate its capability of assisting drivers and improving the safety of automobiles.

### V. DRIVER AUTHENTICATION WITH Wi-Fi

One of the potential threat to automobile safety is that anyone with access to the car key can operate the car. Since automobile driving is a highly demanding activity, driving by an unauthorized or/unqualified driver may increase the chance of car accidents and impose threats to road safety. In this section, we propose a Wi-Fi-based in-car driver

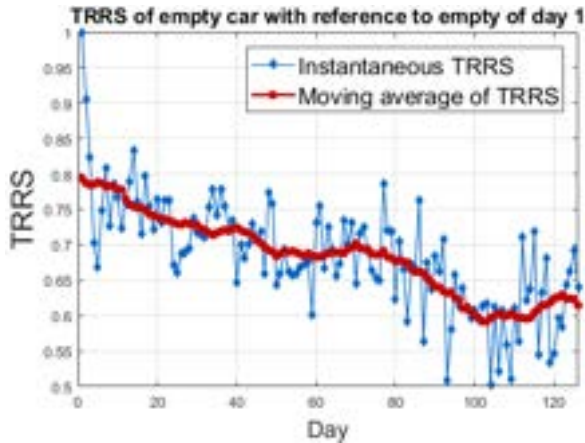


**FIGURE 4.** Demonstration of changes for in-car environment along the time.

authentication/recognition system that can accurately recognize the driver identify, and thus it can serve as a promising security and safety enhancement tool for future smart cars. Driver authentication also aims to facilitate automatic personal adjustment of temperature, seat and mirror positions in the car, based on the identity of the recognized driver.

Radio biometrics is the pattern of a human body introduced to the wireless propagation environment and is determined by the unique biological characteristics of each individual [44]. According to the literature, the wireless propagation around the human body highly depends on the physical characteristic (e.g., height and mass), the total body water volume, the skin condition and other biological tissues. Researchers have studied the relationship between the EM wave absorption of human bodies and the human physical characteristics [43], the interaction of EM waves with biological tissue [42] and the dielectric properties of biological tissues [68], [69]. Hence, considering the combination of all the physical characteristics and other biological features that affect the propagation of electromagnetic waves around the human body and how variable those features can be among different individuals, the radio biometrics is unique for everyone and thus can be used for identifying individuals.

As wireless signals propagate inside the car, the CSI obtained from the in-car Wi-Fi devices has the multipath information characterizing the in-car environment, and the radio biometric information of the driver sitting inside the car will also be recorded in the CSI. In this section, we leverage CSI that contains individual radio biometric information as the sample to identify drivers and use ML techniques to generalize radio biometric information for each driver and overcome the data uncertainty due to noise and dynamics recorded in the CSI. We implement accurate driver identification and verification with commercial Wi-Fi devices in a smart car scenario.

### A. CHALLENGES

The CSI obtained from the commercial Wi-Fi devices has the multipath information characterizing the in-car environment.

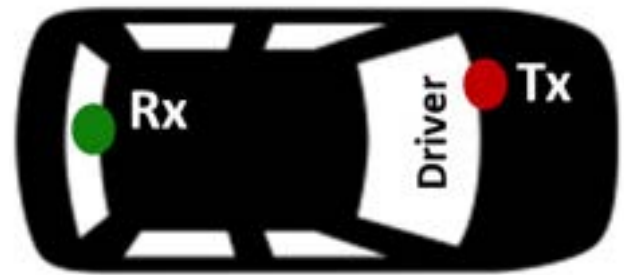


**FIGURE 5.** Location of transceivers in the car.

Since the wireless signal reaches the receiving antenna from more than one path, the human radio biometrics are implicitly embedded in the multipath CSI profile. The human body may only affect a few paths to the multipath CSI, and the energy of those paths is small due to the low reflectivity and permittivity, compared with other static objects such as the walls and furniture. As a result, the human radio biometrics, captured through radio shot [44], are buried by other useless components in the CSI. In other words, the CSI obtained from the radio shot of a person is highly correlated with the environment. In reality, this in-car environment keeps changing with time. Hence, when the in-car environment is altered, the CSI containing the driver radio biometrics is also changed. The proposed system, therefore, should be adaptive to these changes.

In the proposed system, machine learning (ML) models are used to address the problem of “changing in-car environments” using a radio biometric data set. The driver radio biometric data set was built using radio shots of five individuals collected over a period of two months in a car parked at different locations in a public parking lot. The data set is used to understand the dynamics of the in-car environment and its effect on the human radio biometrics. The radio biometrics of each driver is captured with a commercial Wi-Fi devices that are deployed in the car as shown in FIGURE 5.

### B. METHODOLOGY

In the proposed wireless AI driver authentication system, we address the problem of in-car environmental changes. We build the first multiple-driver radio biometric database consisting of radio biometrics of seven people collected over a period of two months. With the help of the database, we integrate ML techniques to make the proposed driver authentication system adaptive to different in-car environments. We present details of the ML techniques we adopted in the following.

#### 1) K-NN

In the proposed in-car driver authentication system, each day a new in-car environment is presented. This new in-car environment can be viewed as a new instance of the problem and instance-based learning methods are an intuitive choice [70]. Among these,  $K$ -nearest neighbor rule is the simplest one and we use it as a baseline for the performance comparison.

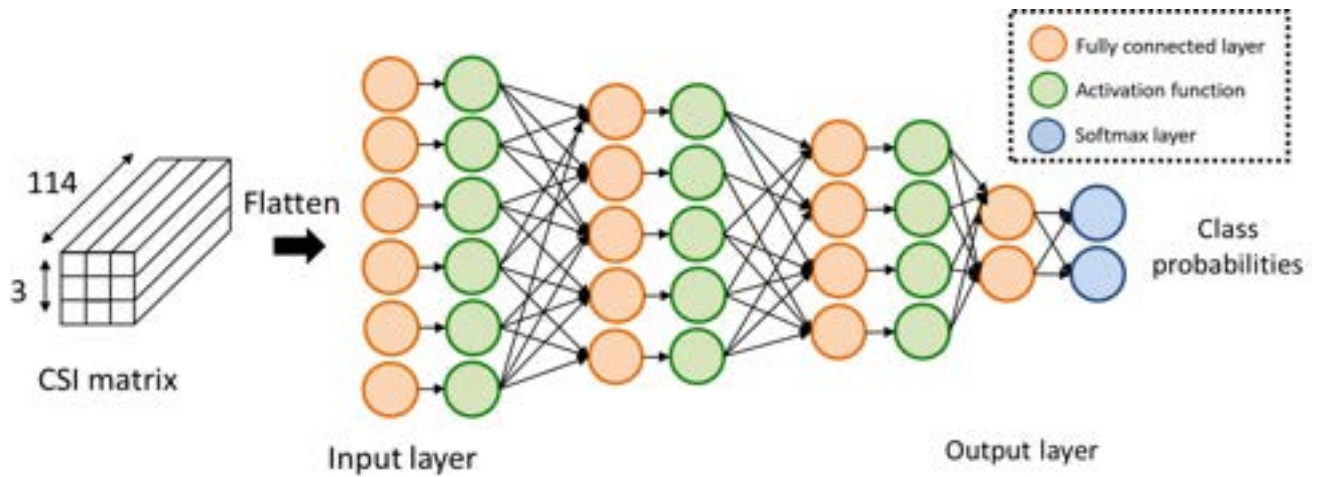


FIGURE 6. Architecture of proposed neural network.

2) SVM

The radio biometric data is high dimensional and is not always linearly separable. Support vector machine (SVM), which belongs to the class of kernel methods, projects the data to a high dimension where it is linearly separable and finds the best hyperplane which can do the classification with maximum margin [71]–[73]. In this article, we evaluate the system using linear and RBF kernels.

3) NN

Neural networks (NN) have been extremely successful in the fields of computer vision, image processing and have a vast variety of applications. We evaluate the proposed in-car driver authentication system using a neural network with two hidden layers and ReLU activation. The architecture of the NN is shown in FIGURE 6. The hyper-parameters are determined using the cross-validation technique.

4) GROUPING

We have seen that the CSI is very sensitive to changes in the in-car environment. Along with the changes in the in-car environment, the variations in the seating position of the driver also causes changes in the received CSI. To make the proposed in-car driver authentication system robust to such changes, we adopt the grouping technique. During the data collection, for each session of the test, four radio shots are recorded with the recording of the empty car CSI in between them. These four radio shots are sent through the ML model to obtain a combined decision. FIGURE 7 explains the grouping technique in a NN. We index the four radio shots as  $i, i = 1, 2, 3, 4$ . In the case of an NN, let  $P_{Ai}$  and  $P_{Bi}$  represent the predicted class probability of the  $i^{th}$  radio shot under class A and class B, respectively. Then the identity of the driver is determined as class A if  $\sum P_{Ai} > \sum P_{Bi}$  and vice versa.

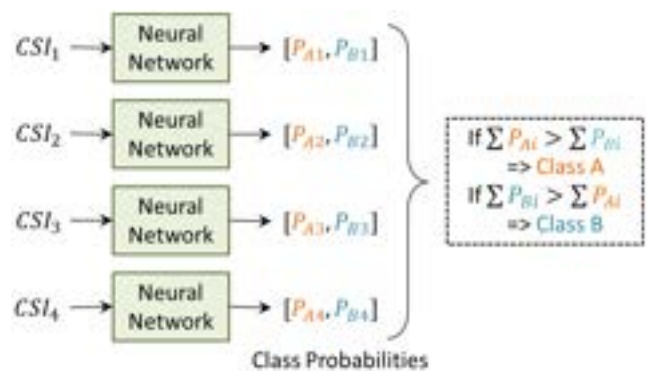


FIGURE 7. Demonstration of the proposed grouping method.

C. EXPERIMENTAL RESULTS

To evaluate the performance of the proposed in-car driver identification system, we build a in-car driver authentication database for a total of 5 test subjects who are addressed as A, B, C, D, and E. We build the system prototype with a pair of commercial Wi-Fi devices. The TX has 2 omnidirectional antennas and the RX has 3 omnidirectional antennas. The CSI, a.k.a. the radio biometrics, is captured when each test subject sits in the driver seat with the carrier frequency being 5.805 GHz and the bandwidth being 40 MHz.

Using the ML models described in the previous section, we evaluate the performance of the proposed system using the in-car driver authentication database. Since the amount of data is limited compared to what most ML methods require, we use the cross-validation technique to report accuracy [74].

1) TWO-DRIVER AUTHENTICATION

In two-driver authentication, we differentiate between two authorized drivers by solving a two class problem. This scenario can serve a similar purpose as the existing memory seating facility in cars and provide driver authentication simultaneously. Table 1 shows the performance of the two-driver authentication using different ML models for all



**TABLE 1.** Performance of two driver authentication.

Classes	K-NN	Linear SVM	SVM-RBF	NN
A-B	86.29	91.67	89.58	89.58
A-C	90.30	92.08	93.39	94.88
A-D	87.66	94.06	92.19	92.79
A-E	88.82	91.87	94.69	94.23
B-C	85.20	86.93	86.40	90.44
B-D	76.70	86.61	86.93	86.60
B-E	85.5	88.85	91.35	91.88
C-D	81.80	86.87	88.80	91.24
C-E	69.08	75.31	74.48	80.40
D-E	80.15	89.22	89.17	91.50

**TABLE 2.** Performance of two driver authentication with grouping.

Classes	KNN	SVM-Linear	SVM-RBF	NN
A-B	86.40	93.75	91.45	96.58
A-C	91.00	94.17	94.17	99.36
A-D	88.81	94.80	93.54	98.08
A-E	89.25	91.46	95.21	99.36
B-C	87.06	89.37	87.91	96.37
B-D	74.12	87.30	89.37	95.51
B-E	85.53	90.62	93.33	94.88
C-D	83.77	85.00	89.17	95.10
C-E	65.57	75.42	73.33	84.19
D-E	80.70	88.75	91.04	96.80

possible sets of two drivers from the database. We can observe that in most cases, the NN performs the best with comparable accuracy to SVM and a significant margin over the *k*-NN accuracy. Table 2 shows the performance of the two-driver authentication using the grouping technique. We can observe that in all the cases, the grouping technique significantly improves the performance of an NN.

The ML models allow the system to become adaptive to changes in the in-car environment. These models require sufficient data to draw inferences and detect patterns in the data. FIGURE 8 shows a moving average of the performance of an NN with an increasing amount of data. The system, therefore, becomes smarter and smarter with time as more and more data points become available.

**D. NOVELTY AND LIMITATION**

The earlier human recognition works were proposed for indoor environment and relied on time-reversal techniques to match similar radio biometrics embedded in the CSI. The proposed driver authentication system first identified the problem of previous work being vulnerable to indoor environment changes through long-term data acquisition and then applied different techniques including SVM and ML algorithms to overcome the environmental changes. Considering the prevalence of cloud storage and cloud computing, the proposed driver authentication system could send CSI back to the cloud

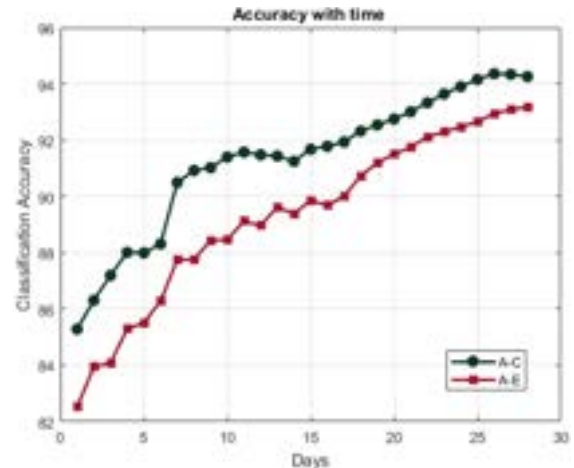


**FIGURE 8.** Performance of smart learning: accuracy grows with time.

for offline training and reload the trained model on the device for classification. Hence, the computation overhead and the delay in terms of identifying a driver should be small.

In this work, we conducted monitoring and experiment on 5 test subjects. On one hand, as the first attempt to propose the idea of identifying drivers in a car using Wi-Fi signals, the current work has been conducted to prove the concept of in-car driver authentication with Wi-Fi. It is difficult to conduct experiments that involve tens and hundreds of test subjects at this very first stage. On the other hand, as in a typical use case of household cars, the number of daily drivers for a car is two, e.g., husband and wife. Even if we consider children as potential drivers, the total number of drivers will most likely be less than 5.

**VI. IN-CAR VITAL SIGN MONITORING WITH Wi-Fi**

As an important metric of vital signs, respiratory rate is the number of breaths one takes per minute and is used as a measurement of the body’s basic functions for assessing the general physical health of a person. The normal respiration rate for an adult is generally between 12 and 20 breaths per minutes (BPM). One tends to have a lower BPM during relaxation, whereas performing demanding cognitive tasks could affect his respiration rate, e.g., lead to a higher than normal BPM [75]. Breathing rate is an important vital sign indicating the health status for both the driver and the passengers. Conventional approaches to measuring the breathing rate involve a flow sensor to be put close to one’s nose/mouth or a belt sensor to wrap one’s chest, which may affect the driving performance severely due to their uncomfortable, disturbing and distracting nature.

Not only can CSI capture environmental perturbations due to macro human activities and radio biometrics, but it can also record subtle changes introduced by human respiration. The breathing induced chest movement introduces a periodic perturbation to the wireless propagation. Hence, because of its periodic pattern recorded by the wireless signals, the human breathing information can be extracted with high fidelity from



the CSI time series. In this section, we present the wireless AI vital monitoring system for a smart car scenario that tracks the breathing rate for the driver and the passengers and monitors their well-being.

### A. CSI MODEL UNDER BREATHING IMPACT

To better understand the impact of breathing on CSI, we start with a time-varying channel frequency response (CFR) model. In the presence of propagation perturbations caused by chest movement, the CFR of the  $m$ -th link at time  $t$  is modeled as

$$\mathbf{h}_T^{(m)}(t, f_k) = \sum_{l=1}^L a_l(t) \exp(-j2\pi f_k \frac{d_l(t)}{c}) + n(t, f_k), \quad (3)$$

where  $k \in \mathcal{V}$  is the subcarrier index with center frequency  $f_k$  in the set of usable subcarriers  $\mathcal{V}$ , and the number of accessible subcarriers is  $N_{sc}$ .  $L$  is the total number of multipath components (MPCs), while  $a_l(t)$  and  $d_l(t)$  denote the complex gain and propagation length of MPC  $l$ .  $c$  is the speed of light and  $n(t, f_k)$  is the additive white Gaussian noise. For the system with multiple antennas, there are  $N_{TX} * N_{RX}$  links in total, where  $N_{TX}$  and  $N_{RX}$  is the number of transmitter antennas and receiver antennas respectively.

Due to the perturbation introduced by breathing, gains and delays of one or more multipaths change along the time and the CFR exhibits periodic variation. In the following analysis, we consider the case when there is one person sitting in the car whose breathing cycle is  $T_b$  seconds. Later, we will show that the single subject vital monitoring can be easily extended to a multiple-person case.

The MPCs in (3) can be classified into two sets:  $\Omega_s$  and  $\Omega_d$ .  $\Omega_s$  denotes the set of time-invariant MPCs and  $\Omega_d$  denotes the set of time varying MPC, due to the reflection and scattering of the human body. Thus, the gain of MPCs in  $\Omega_d$  can be modeled as [41]

$$a_l(t) = a_l \times (1 + \frac{\Delta d_l}{d_l} \sin\theta \cdot \sin(\frac{2\pi t}{T_b} + \phi))^{-\Psi}, \quad (4)$$

where  $a_l$  and  $d_l$  represent the gain and the path length of the MPC without breathing impact,  $\Delta d_l$  denotes the additional positional displacement (a.k.a., path length difference) of the MPC in  $\Omega_d$  caused by the chest movement due to breathing,  $\theta$  is the angle of incidence between the human body and the EM wave,  $\phi$  indicates the initial phase of breathing, and  $\Psi$  is the path loss exponent. Since the path length difference due to chest movement is much smaller than the path length, i.e.,  $\Delta d_l \ll d_l$ , we can approximate the MPC gain  $a_l(t)$  with the time-invariant MPC gain  $a_l$ .

### B. BREATHING RATE ESTIMATION

In the proposed system, we utilize the CSI amplitude information to model the breathing signal recorded by the wireless propagation, considering that the phase of  $\mathbf{h}_T^{(m)}(t, f_k)$  is corrupted by the phase noise caused by timing and frequency synchronization offset in the real measurement. Given the

periodic chest movement introduced by breathing, we can have

$$|\mathbf{h}_T^{(m)}(t, f_k)| = g(f_k)b(t - \Delta t_{f_k}), \quad (5)$$

where  $g(f_k)$  denotes the channel gain and  $\Delta t_{f_k}$  represents the initial phase of the breathing signal  $b(t)$  on the subcarrier with a center frequency  $f_k$ .

Although the channel profile exhibits a periodic pattern when there exists only one person in the coverage area, it is not straightforward to analyze the periodicity in the time-domain breathing signal for the multi-people case. We develop a method to estimate multiple breathing rates from the frequency spectrum of  $|\mathbf{h}_T^{(m)}(t, f_k)|$ , because the frequencies of multiple individuals' breathing can be isolated in the frequency domain. In particular, our system analyzes the time series of CFR amplitude on each subcarrier in the frequency domain by using power spectrum density (PSD). In addition, since the breathing rate is limited in a certain range, a band-pass filter is applied over the frequency spectrum to enhance the estimation accuracy. The steps are described as follows.

- 1) *Fourier Transform*: We first apply a sliding window of length  $W * F_s$  to the captured CSI time series on the time domain, and then obtain the frequency spectrum by performing a fast Fourier Transform (FFT) over each time window. Here,  $F_s$  is the sounding rate, and  $W$  is the window length in seconds. FIGURE 9 demonstrates an exemplary PSD of 3 breathing signals recorded in a 60-second CSI time window. In FIGURE 9, the x-axis denotes the Fourier frequency index (a.k.a., BPM), the y-axis represents the subcarrier index, and different color represents the energy of the PSD.
- 2) *Subcarrier Selection*: The sensitivity of each subcarrier to different breathing signals is different as shown in FIGURE 9, where different subcarriers exhibit different PSD values for the same breathing frequency. To get a better breathing rate estimation, for each frequency indexes (a.k.a., BPM), we select the subcarrier with the highest signal-to-noise ratio (SNR), i.e., picking the subcarrier whose PSD value is above a pre-selected threshold. After selecting the best subcarriers for all frequency components, the total spectrum energy of each link is normalized to 1. At the end of this step, each heat-map in FIGURE 9 is projected to a 2-D PSD plot as shown in FIGURE 10.
- 3) *Link Combination*: As demonstrated in FIGURE 10, different TX-RX links have different quality and are sensitive to different breathing signals. To further boost the breathing estimation accuracy, we fuse the information from all TX-RX links and obtain the final PSD by summing up the normalized spectrum energy of each frequency component on different links. An example is given in FIGURE 11, where information from all subcarriers and TX-RX links captured in the same CSI time window is fused into one PSD plot.

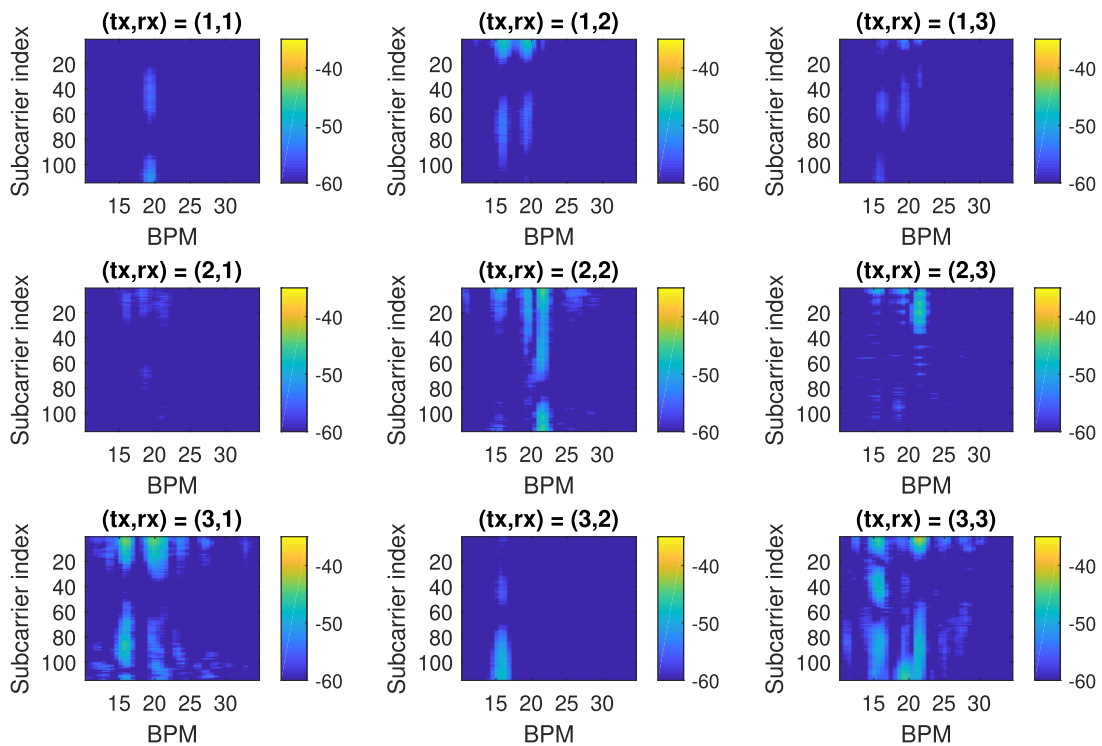


**FIGURE 9.** The PSD of breathing signals on all subcarriers over different TX-RX links calculated from a 60-second CSI time series. The title of each subplot  $(tx, rx) = (i, j)$  indicates the link between the  $i$ -th TX antenna and the  $j$ -th RX antenna. The CSI is captured through a 3-by-3 MIMO transmission under 10 Hz sounding rate with ground truth being 3 people in a car.

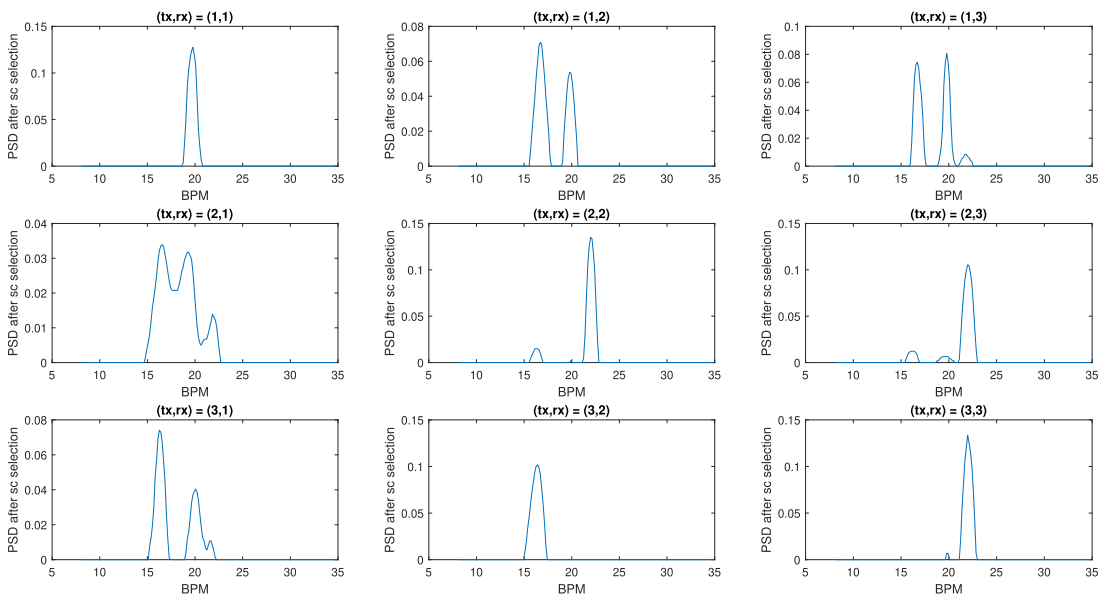


**FIGURE 10.** The PSD of breathing signals after subcarrier selection over different TX-RX links with the title  $(tx, rx) = (i, j)$  indicating the link between the  $i$ -th TX antenna and the  $j$ -th RX antenna (Ground truth being 3 people in a car).

4) *Peak Detection:* After getting the PSD plot as shown in FIGURE 11 for each time window, we can obtain the final spectrogram by concatenating the PSD of different windows along the time axis. An example of the final spectrogram of breathing signals is depicted in FIGURE 12 and the CSI is captured when 3 test

subjects are sitting in the car. We can extract the breathing rate from the spectrogram by selecting the first strongest  $m$  peaks in the PSD for each time instance, where  $m = \min\{M, M'\}$  is the minimum number between the maximum passenger capacity  $M$  and the number of peaks  $M'$  whose spectrum strength is above

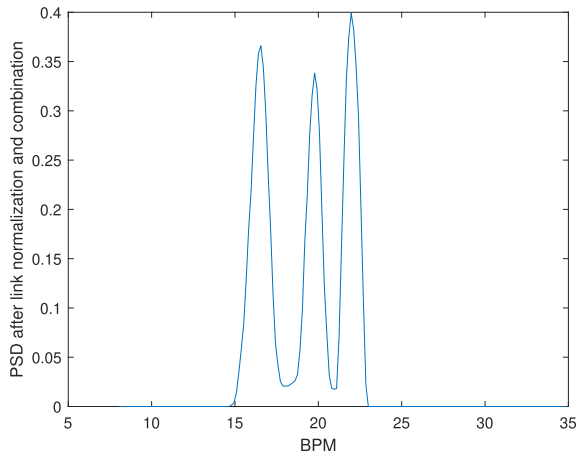


**FIGURE 11.** The PSD of breathing signals after TX-RX link combination and normalization and three BPM energy peaks can be observed (Ground truth: 3 subjects in car).

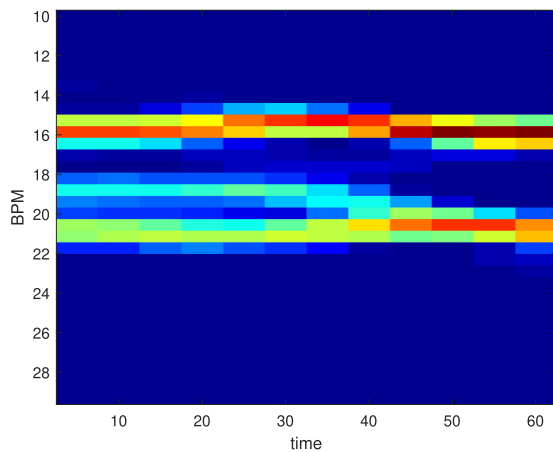


**FIGURE 12.** The final spectrogram of breathing signals extracted from the 60-second CSI time window (Ground truth: 3 subjects in car).

a predefined energy threshold. The estimated breathing rates correspond to the BPM indexes of the selected peaks.

### C. EXPERIMENTAL RESULTS

To evaluate the performance of breathing monitoring, we monitor the breathing rate of multiple people and compare the breathing rate estimation with the ground truth. The breathing signals of test subjects are monitored and captured using a pair of commercial Wi-Fi devices. We deploy the TX and the RX as shown in FIGURE 5 and the prototype transmits over the 5-GHz Wi-Fi band under a 40 MHz bandwidth and a 30 Hz sounding rate.

Denote the ground truth of person  $i$ 's breathing rate as  $b_i$  and we assume individual breathing rate is constant during the test. We keep monitoring and collecting the CSI for a duration of  $T$  and apply a sliding window with length  $W$  over the CSI time series. The stride between consecutive CSI windows is  $W_s$ . For each window, a breathing rate estimation

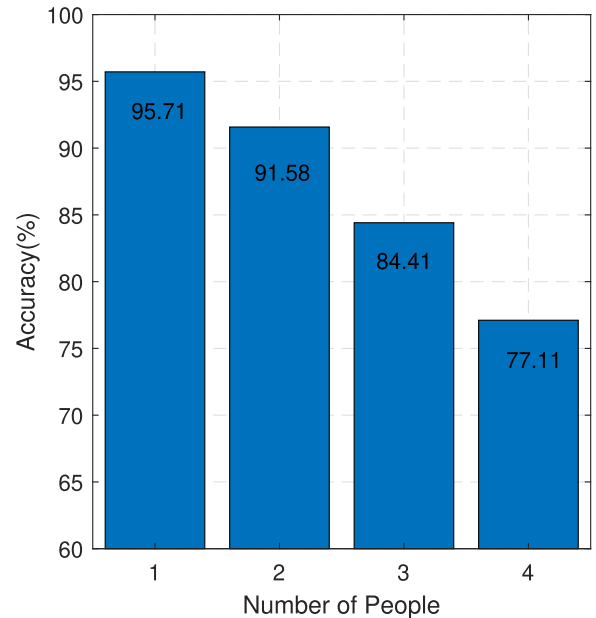


**FIGURE 13.** Accuracy of breathing estimation with different number of people simultaneously in the car.

is obtained and thus in total we have  $I = \lfloor \frac{T-W}{W_s} \rfloor + 1$  estimations for the CSI series of length  $T$ .

The accuracy of estimation is defined as

$$Accuracy = \left( 1 - \frac{1}{I \times N} \sum_{i=1}^I \sum_{n=1}^N \left| \frac{b_{n,i} - b_n}{b_n} \right| \right) \times 100\%, \quad (6)$$

where  $I$  is the total number of breathing estimations,  $N$  is the total number of test subjects, and the breathing estimation for the  $n$ -th test subject in the  $i$ -th window is denoted as  $b_{n,i}$ , given his/her ground truth breathing rate as  $b_n$ .

As shown to FIGURE 13, up to 4 people are invited into a car for vital sign monitoring. The accuracy for breathing estimation when only 1 test subject is in the car is about 96%. The accuracy drops as the number of people increases. This is because the breathing strength of some test subjects may be much smaller than that of others' breathing signal at some time instances, i.e., the SNR of the weak breathing signal is significantly lower than others. Consequently, the proposed system may fail to decode that weak breathing signal, leading to a miss detection.

### VII. IN-CAR PASSENGER COUNTING WITH WI-FI

Accurate and reliable crowd counting that estimates the number of people in a given environment is important for future smart car application. For instance, the control panel can automatically adjust the ventilation based on the occupancy level, which can decrease the energy consumption for the car. In-car passenger counting also enhances automobile safety in that it can support smart in-car safety functionality like activating airbags based on the number of passengers in the car.

Nowadays, crowd estimation is mainly based on the video signal, which compromises user privacy. Although there are a few works using RF signal to estimate the number of people, their approaches are mainly based on relationship between the number of moving people and the variation of CSI, which is invalid for the smart car environment, where people are sitting quasi-statically. Inspired by the in-car breathing rate estimation system presented in Section VI, we propose a wireless AI crowd counting system that can extract distinct traces of independent vital signals and thus estimate the number of people. The proposed system provides a solution to future smart car passenger counting based on the RF signal in a car.

Specifically, as the Wi-Fi device keeps sensing the in-car environment, the obtained time series of CSI contains the breathing signals of each individual in a car. The rate of a breathing signal at a specific time stamp can be estimated by means of the vital sign estimation algorithm described in Section VI. In this part, we will present a dynamic programming based tracking algorithm, which is capable of iteratively separating and recognizing the trace of estimated breathing rate of different individuals, and thus counting the number of people in a car. The details are as follows.

#### A. THE MARKOV CHAIN MODEL FOR HUMAN BREATHING

Human breathing introduces a periodic signal which smoothly changes over time. Based on the fact we state in Section VI, a person's continuous breathing should correspond to a smooth trace in the frequency spectrum extracted from the CSI time series, as demonstrated in FIGURE 12. Thus, the crowd estimation problem can be solved by determining how many traces exist in the observation time.

When there are multiple persons in the same wireless propagation environment, there will be multiple breathing rate traces existing in the same spectrogram, as shown in FIGURE 12. In order to resolve multiple breathing rate traces captured by the wireless signal, we propose an iterative algorithm that repeatedly identifies the most significant breathing rate trace from the current spectrogram and then eliminates the identified trace from the spectrogram until there is no breathing rate trace remained. To demonstrate the proposed algorithm, we start with a single trace scenario.

Let  $S \in \mathbb{R}_+^{I \times J}$  be the frequency spectrogram obtained from the CSI time series.  $I$  denotes the total number of breathing rate estimations along the time,  $I = \lfloor (T - W) / W_s \rfloor + 1$ , where  $T$  denotes the total length of CSI time series,  $W$  represents the length of sliding window for calculating FFT, and  $W_s$  is the stride of the sliding window.  $J$  denotes the total number of discrete frequencies whose resolution is determined by the CSI sounding frequency and the number of FFT points. Moreover, a breathing rate trace  $\mathbf{f}$  on the spectrogram  $S$  can be expressed as a sequence of estimated breathing rates, i.e.,  $\mathbf{f} = \{f(i)\}_{i=1}^I$ , where  $f(i)$  represents the estimated breathing rate at the given time stamp  $i$ . Let  $S(i, f(i))$  denote the spectrum strength of the estimated breathing rate  $f(i)$ , the total energy

of a trace is defined as the total sum of the spectrum strengths of estimated breathing rate, i.e.,  $E(\mathbf{f}) = \sum_{i=1}^I S(i, f(i))$ .

Given a spectrogram obtained from the CSI time series, there might be an infinite number of candidate traces. However, the trace that corresponds to the real human breathing captured through wireless propagation should have a higher energy  $E(\mathbf{f})$  compared to other frequency traces. For a given spectrum  $S$ , we define the dominant breathing rate trace  $\mathbf{f}^*$  as the trace with the highest energy among all possible traces  $\mathbf{f}$ , i.e.,

$$\mathbf{f}^* = \arg \max_{\mathbf{f}} E(\mathbf{f}). \quad (7)$$

On the other hand, because the breathing rate of a human cannot change abruptly, the estimated breathing rate trace should be smooth and the estimated breathing rate at current time instance should be highly dependent on the breathing rate at the previous time stamp. In practice, because the frequency resolution of FFT is restricted by the length of the CSI window where FFT is performed, we can only get discrete frequency readings on the spectrogram. Hence, considering the nature that human breathing is continuous and the finite frequency resolution, we adopt the Markov chain to model the transition of subsequent breathing rate estimations. We assume the current breathing rate estimation only depends on the previous breathing rate estimation. The details are as follows.

We denote the difference of human breathing rates between adjacent time instances as  $\delta f$  and assume it follows the Gaussian distribution as  $p(\delta f) \sim \mathcal{N}(0, \sigma^2)$ . The breathing rate estimation obtained from the proposed algorithm in Section VI follows the transition probability as  $P(j, j') = p(f(i) = j' | f(i-1) = j)$ , where  $P(\cdot, \cdot)$  represents the Markov transition probability and  $P(j, j')$  denotes probability of the transition from the breathing rate of  $j$  at time stamp  $i-1$  to  $j'$  at the next time stamp  $i$ .  $P(j, j')$  can be obtained by  $\int_{(j'-j-\frac{1}{2}) * \Delta f}^{(j'-j+\frac{1}{2}) * \Delta f} p(\delta f) \mathbf{d}\delta f$ .

As we discussed above, on one hand, the optimal breathing rate trace should be the trace of the highest spectrum energy. On the other hand, we add a regularization term to ensure the continuousness and smoothness of the estimated breathing rate trace. Finally, we propose the single breathing rate trace identifying and tracking problem as

$$\mathbf{f}^* = \arg \max_{\mathbf{f}} G(\mathbf{f}), \quad (8)$$

where the objective function is defined as  $G(\mathbf{f}) = E(\mathbf{f}) + \lambda \left\{ \log(\pi(f(1))) + \sum_{i=2}^I \log(P(f(i-1), f(i))) \right\}$ ,  $\pi(f(1))$  represents the initial probability of the first breathing estimation being  $f(1)$  which is proportional to its spectrogram energy, and  $\lambda$  denotes the coefficient for regularization.

#### B. CROWD ESTIMATION

It worths noting that the original objective function  $G(\mathbf{f})$  can be decoupled as  $G(\mathbf{f}) = G(\mathbf{f}') + S(I, f(I)) + \log(P(f(I-1), f(I)))$ , where  $\mathbf{f}' = [\mathbf{f}', f(I)]$ . In other words, given the



current breathing rate estimation  $f(I)$ , the optimal trace  $\mathbf{f}$  ahead of  $f(I)$  can be easily obtained by maximizing  $\left\{G(\mathbf{f}') + \log\left(P(f'(I-1), f(I))\right)\right\}$ .

Inspired by that, we propose to utilize the dynamic programming (DP) to solve the breathing rate trace optimization problem defined in (8) and define the utility of the current estimated breathing rate trace arrives at rate  $f(i) = j$  at time instance  $i$  as

$$g(i, j) = S(i, j) + \max_{j'} \left\{ g(i-1, j') + \lambda \log(P(j', j)) \right\}, \quad (9)$$

By maximizing the utility function  $g(i, j)$  for every pair of  $(i, j)$  as we traverse through all time indexes  $i$ 's and breathing rate  $j$ 's, we break down the original optimization problem into a sequence of optimization problems and ensure that  $g(i, j)$  represents the maximal utility we can have if the breathing rate trace stops at  $(i, j)$  on the spectrogram. The optimal breathing rate trace should end at the breathing rate  $f^*(I)$ ,  $f^*(I) = \max g(I, j), j = 1, 2, \dots, J$  and we can obtain the optimal breathing rate trace by performing a standard backward search given  $f^*(I)$ .

Each round of the aforementioned DP approach locates and returns the strongest trace in the spectrum. We can resolve all the breathing rate traces of a multiple-person breathing application by performing the DP iteratively. Particularly, for a given spectrogram of breathing signals extracted from the CSI time series, we first calculated the utility function in (9) for the obtained spectrogram to determine whether nobody is in the space. When someone is inside the monitoring space, the energy of the corresponding breathing rate trace will be detected, i.e.,  $g(I, j) > 0, \exists j$ . If one or more breathing signals are detected, the proposed method will return the strongest breathing rate trace with DP and clean its energy from the spectrogram afterward. The proposed method iteratively performs the trace finding and nulling procedure until no breathing rate trace energy detected. The diagram of the proposed algorithm is plotted in FIGURE 14.

By tracking the number of distinct breathing rate traces in the spectrogram extracted from the CSI time series, we can infer the number of people in the environment. To further improve the accuracy of breathing rate tracking, we utilize the time diversity from consecutive sliding windows to update breathing rate traces, considering consecutive windows share the same CSI subsequence of length  $W - W_s$ . If a breathing rate trace from the current sliding window overlaps with the one in the previous window, two traces belong to the same person, and we can substitute the corresponding segment of the previous breathing rate trace with the current one in the current time window. If the current trace cannot merge with any of the breathing rate traces in the previous window, a new breathing rate trace is found indicating one more person being detected in the monitoring space. Hence, the number of people in a car,  $M$ , in a particular time slot can be estimated as the number of breathing rate traces exhibited in the spectrogram at that time.

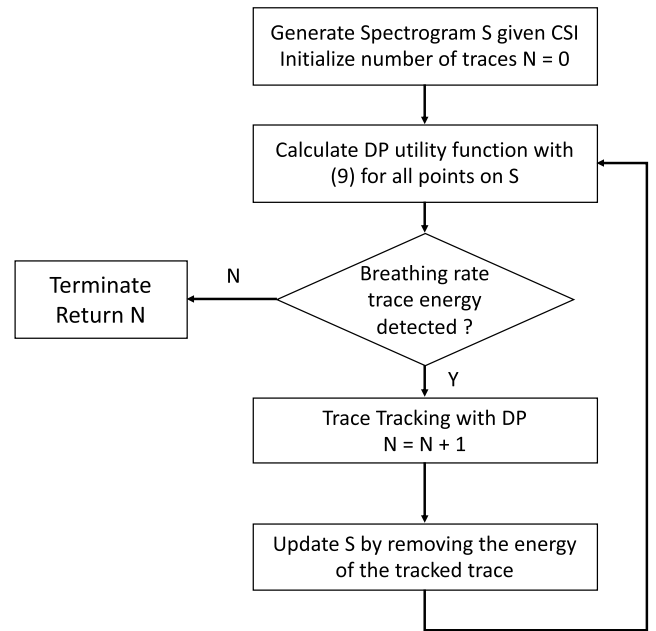


FIGURE 14. The diagram of the proposed iterative DP breathing rate trace tracking algorithm.

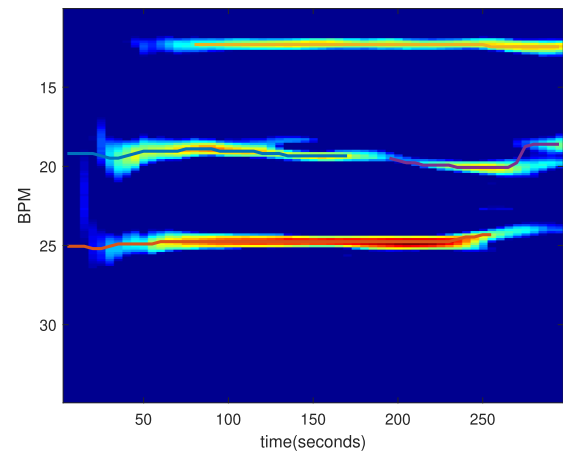


FIGURE 15. An example of multiple breathing rate traces tracking with the proposed iterative DP breathing rate trace tracking algorithm. Three breathing rate traces are marked and tracked in the spectrogram (Ground truth: 3 people in a car).

We demonstrate an example of breathing rate trace tracking using the proposed iterative DP approach in FIGURE 15, where three breathing rate traces are tracked in the spectrogram. The CSI time series is captured for 300 seconds under a 30 Hz sounding rate when there are 3 people sitting in a car. The window length  $W$  is set to 60 seconds and the stride length of consecutive windows is 5 seconds. The x-axis is the time index and the y-axis is the BPM frequency index.

### C. EXPERIMENTAL RESULTS

To evaluate the performance of the proposed algorithm, we capture the CSI time series and monitor the in-car environment when there are up to 4 test subjects sitting in the car

1	93.5%	6.5%	0.0%	0.0%
2	1.4%	87.9%	10.6%	0.0%
3	3.9%	15.5%	73.5%	7.1%
4	0.0%	5.4%	23.9%	70.7%
	1	2	3	4
	Predicted Number of People in the Car			

**FIGURE 16.** Confusion matrix of people counting using the proposed iterative DP algorithm.

and being monitored for 300 seconds. We build the system prototype with a pair of commercial Wi-Fi devices that perform the 3-by-3 MIMO transmission under a 30 Hz sounding rate over the 5 GHz band and deploy the TX and RX in the car under the setting in FIGURE 5. The window length  $W$  of each CSI sliding window is set to 60 seconds and the stride length of consecutive windows is 5 seconds. By performing the proposed iterative DP algorithm as depicted in FIGURE 14 to the captured CSI time series, the breathing rate traces of the test subjects in the car can be obtained and thus the number of people can be estimated.

FIGURE 16 shows the confusion matrix of people counting using the proposed iterative DP algorithm, where the number in the cell on the  $i$ -th row and the  $j$ -th column represents the percentage of time that the proposed system estimates the number of people in a car as  $j$  when the ground-truth number is  $i$ . The estimation accuracy achieves 93.5% when only one test subject is sitting in a car. In general, over 94.6% of the time and for all four cases as listed in FIGURE 16, the proposed wireless AI passenger counting system can estimate the ground-truth number of people within  $\pm 1$  number of people error.

### VIII. IN-CAR CHILD PRESENCE DETECTION WITH WI-FI

According to the statistics in [54], it is extremely dangerous and can be fatal for a child if he/she was left in a closed car without parents attendance. However, there is currently no reliable techniques based on cameras or pressure sensors that can detect child presence in a car, because most of the kids are put inside a car seat on the back seat facing to the back of the car and their weight is light. Hence, it is critical and urgent to develop in-car monitoring systems that can detect a child promptly when he/she is left inside a locked car even with obstruction and thus avoid such a tragedy.

As demonstrated by the Wi-Fi based vital monitoring and passenger counting systems discussed in the previous sections, people sitting in a car will introduce perturbations to the in-car wireless propagation environment. On one hand,

vital signals such as breathing will bring minor but periodic CSI patterns. On the other hand, human movements will add irregular changes into the CSI that make the consecutive CSI estimations at the receiver side distinct and less correlated. Inspired by that, in this section, we propose a novel Wi-Fi-based CPD algorithm that utilizes the information in a CSI time series to detect the presence of a living child.

#### A. STATISTICAL MODELING OF CSI MEASUREMENTS

Considering a pair of TX and RX being deployed in a car environment and equipped with omnidirectional antennas, the TX emits a continuous EM wave via its antennas, which is received by the RX, and the received electric field is denoted as  $\mathbf{E}_{RX}(t, f)$ . We define the power response of the corresponding CSI as  $g(t, f)$ ,

$$g(t, f) \triangleq |h(t, f)|^2 = \mu(t, f) + \varepsilon(t, f), \quad (10)$$

where  $h(t, f)$  denotes the measured CSI on subcarrier  $f$  at time  $t$ ,  $\mu(t, f)$  denotes the part contributed by the propagations of the EM waves, and  $\varepsilon(t, f)$  denotes the measurement noise which is an independent additive white Gaussian noise for any subcarriers.

The  $\mu(t, f)$  measures the power of  $\mathbf{E}_{RX}$ , i.e.,  $\mu(t, f) = \|\mathbf{E}_{RX}(t, f)\|^2$ , where  $\|\cdot\|$  denotes the Euclidean norm. Within a sufficiently short period, the received electric field  $\mathbf{E}_{RX}(t, f)$  can be decomposed into: 1) the  $\bar{E}_s(f)$  contributed by all the static scatterers and 2) the  $\bar{E}_d(f)$  contributed by all the dynamic scatterers. By detecting the variations in the received power response  $g(t, f)$ , one can also detect the occurrence of dynamic changes happening in the environment. The details are as follows.

As  $\mu(t, f)$  is due to the propagation of EM waves and  $\varepsilon(t, f)$  is due to the imperfect measurements of CSI, it can be shown through experimental results that  $\mu(t, f)$  and  $\varepsilon(t, f)$  are uncorrelated with each other. Therefore, the auto-covariance function of  $g(t, f)$ , i.e.,  $\gamma_g(\tau, f)$ , can be expressed as

$$\begin{aligned} \gamma_g(\tau, f) &\triangleq \text{cov}(\mu(t, f) + \varepsilon(t, f), \mu(t - \tau, f) + \varepsilon(t - \tau, f)) \\ &= E_d^2(f) \rho_\mu(\tau, f) + \sigma^2(f) \delta(\tau), \end{aligned} \quad (11)$$

where  $E_d^2(f)$  denotes the variance of  $\mu(t, f)$ ,  $\delta(\cdot)$  is Dirac delta function and  $\rho_\mu(\tau, f)$  represents the the auto-correlation function (ACF) of  $\mu(t, f)$ . An important observation is provided in [17] based on the derivation of  $\mu(t, f)$  that when  $\tau \rightarrow 0$ ,  $\rho_\mu(\tau, f) \rightarrow 1$ . The corresponding ACF of  $g(t, f)$  can thus be expressed as [17]

$$\rho_g(\tau, f) = \frac{E_d^2(f)}{E_d^2(f) + \sigma^2(f)} \rho_\mu(\tau, f), \quad (12)$$

where  $\tau \neq 0$ . When there exists motion and  $\tau \rightarrow 0$ , with the knowledge of  $\rho_\mu(\tau, f) \rightarrow 1$ , we know  $\rho_g(\tau, f) \rightarrow \frac{E_d^2(f)}{E_d^2(f) + \sigma^2(f)} > 0$ ; when there is no motion and  $\tau \rightarrow 0$ , we have  $\rho_g(\tau, f) = 0$  since  $E_d^2(f) = 0$ . Therefore,  $\lim_{\tau \rightarrow 0} \rho_g(\tau, f)$  is a good indicator of the presence of motion in the car.

We will exploit this important observation in the following design of CPD.

## B. DESIGN OF CPD ALGORITHM

### 1) MOTION STATISTICS

In practice,  $\lim_{\tau \rightarrow 0} \rho_g(\tau, f)$  cannot be measured directly, because  $\tau \rightarrow 0$  is difficult to achieve due to finite channel sampling rate  $F_s$ . Instead, we use the quantity  $\rho_g\left(\tau = \frac{1}{F_s}, f\right)$  as an approximation as long as  $F_s$  is large enough. Then, we define the *motion statistic* from the CSI power response  $g(t, f)$  as the sample ACF of  $g(t, f)$ , i.e.,

$$\hat{\phi}(f) = \frac{\hat{\gamma}_g\left(\tau = \frac{1}{F_s}, f\right)}{\hat{\gamma}_g(\tau = 0, f)}, \quad (13)$$

where  $\hat{\gamma}_g(\tau, f)$  denotes the sample auto-covariance function of  $g(t, f)$  [76]. When there is no motion, according to the large sample theory [76], the distribution of  $\hat{\phi}(f)$  will converge to an asymptotically normal (AN) distribution  $\mathcal{N}\left(-\frac{1}{T}, \frac{1}{T}\right)$ , where  $T$  denotes the the number of samples. In addition,  $\hat{\phi}(f_1)$  of subcarrier  $f_1$  and  $\hat{\phi}(f_2)$  of subcarrier  $f_2$  are independent and identically distributed (i.i.d.) for  $\forall f_1 \neq f_2$ . Hence, when there exists motion in the measured environment,  $\hat{\phi}(f)$  converges to  $\frac{E_d^2(f)}{E_d^2(f) + \sigma^2(f)}$  as  $F_s \rightarrow \infty$  and  $T \rightarrow \infty$ .

### 2) DETECTION RULE

Based on the previous observations, the distribution of the proposed motion statistics can be summarized as:

$$\begin{aligned} \text{No motion : } & \hat{\phi}(f) \sim \mathcal{N}\left(-\frac{1}{T}, \frac{1}{T}\right), \quad \forall f \in \mathcal{F}, \\ \text{With Motion : } & \hat{\phi}(f) \rightarrow \frac{E_d^2(f)}{E_d^2(f) + \sigma^2(f)} > 0, \quad \forall f \in \mathcal{F} \end{aligned} \quad (14)$$

We define the average of motion statistics as  $\hat{\psi} = \frac{1}{F} \sum_{f=1}^F \hat{\phi}(f)$ , where  $F$  denotes the total number of available subcarriers and  $\hat{\phi}(f)$ 's are i.i.d. for different subcarriers  $f$ . We can then have  $\hat{\psi} \sim \mathcal{N}\left(-\frac{1}{T}, \frac{1}{FT}\right)$ , that is, the variance of  $\hat{\psi}$  is inversely proportional to the number of samples  $T$  and the number of subcarriers  $F$ .

Meanwhile, since the average of motion statistic  $\hat{\phi}(f)$  is a positive number when there is motion in the environment, a simple **detection rule** is proposed for the detection of the presence of motion: given a preset threshold  $\eta$ , if  $\hat{\psi}$  is greater than or equal to  $\eta$ , then the proposed CPD algorithm reports a detection of motion; otherwise, no motion is detected.

*Remark 1:* Based on the characteristics of  $\hat{\phi}(f)$ , the probability of false alarm under a given preset threshold  $\eta$  can be approximated as

$$P_{\mathcal{H}_0}(\hat{\psi} > \eta) = Q\left(\sqrt{FT}\left(\eta + \frac{1}{T}\right)\right), \quad (15)$$

where  $Q(\cdot)$  denotes the Q-function, the tail probability of the standard normal distribution.

For the detection probability of the proposed motion detection algorithm, it is hard to characterize it theoretically since  $\hat{\phi}(f)$  is determined by the location of motion and the working condition of the Wi-Fi chipsets. However, when there is no

motion, the statistical behavior of  $\hat{\psi}$  is only a function of  $F$  and  $T$ , which is independent of the variance of the measurement noise.

However, in practice, the motion near the car may also trigger the detector, which causes undesirable false alarms for the presence detection. To cope with this practical scenario, we utilize the following key observations to improve the performance of the proposed CPD algorithm:

- 1) The motion statistics caused by the motion outside the car are usually very small, while the motion statistics caused by the motion inside the car are much stronger;
- 2) The duration of the motion outside the car is usually very short, which are mainly introduced by the pedestrians or cars passing by.

In the following, we propose an improved **CPD algorithm** which incorporates the above key observations.

Let  $\hat{\psi}[n]$  denote the obtained motion statistic at the  $n$ -th time slot, and given two preset thresholds  $\eta_1$  and  $\eta_2$ , where  $\eta_1 > \eta_2$ , the presence of motion is detected when  $\hat{\psi}[n] > \eta_1$  or  $\frac{1}{W} \sum_{i=0}^{W-1} \hat{\psi}[n-i] < \eta_2$ , where  $W$  stands for the length of the moving average window.

## C. EXPERIMENTAL RESULTS

We build a real-time CPD system using a pair of commercial Wi-Fi devices, one as TX, equipped with 2 omnidirectional antennas, and the other as RX, equipped with 3 omnidirectional antennas, and each link over a pair of antennas has a total of 114 subcarriers.

By default, the system works on channel 161 with a carrier frequency of 5.805 GHz and a bandwidth of 40 MHz. The sampling rate of channel measurements of the devices is set to 30 Hz. We deploy the RX near the on-board diagnostics (OBD) location, which is left of the steering wheel and underneath the dashboard, of a typical sedan, and the TX is placed in two different locations for evaluation:

- Setting #1: the TX is placed underneath the right-front seat;
- Setting #2: the TX is placed above the right-rear seat.

To evaluate the performance of the proposed algorithm, we collect CSI data for different scenarios under each of the two settings:

- Scenario #1: one person sleeps in the car on different seats;
- Scenario #2: one person stays in the car with small motion, e.g., moving head, hands, and legs;
- Scenario #3: several people continuously walks around the car within 2 meters;
- Scenario #4: the car is empty and no one is around the car.

Scenario #1–#2 are target events that the CPD algorithm should detect, while Scenario #3–#4 are the events that should not be detected. For each setting, we collect the data lasting for 25 minutes for Scenario #1–#2 and the data lasting for 15 minutes for Scenario #3–#4.

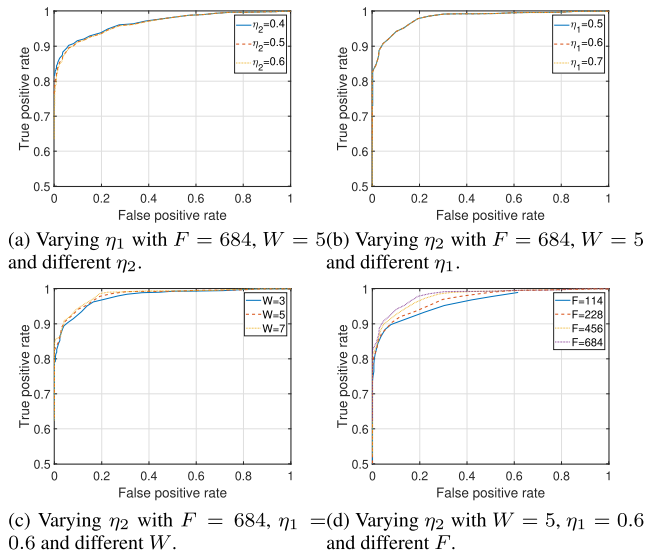


FIGURE 17. The ROC curves for Setting #1.

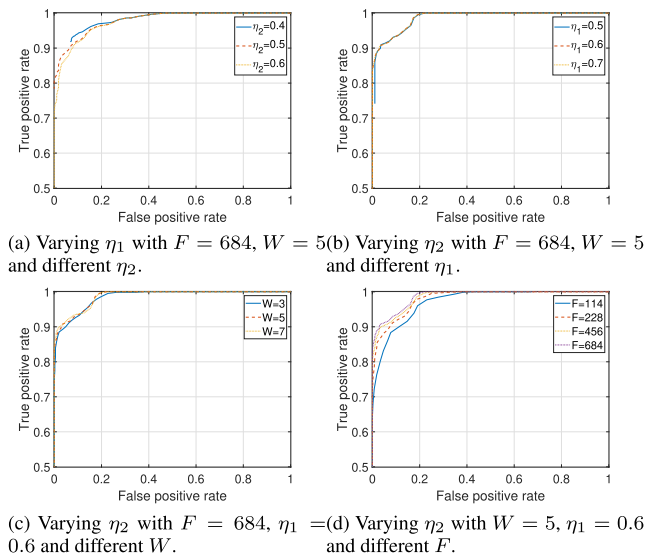


FIGURE 18. The ROC curves for Setting #2.

The proposed algorithm reports a decision for every second and the receiver operating characteristic (ROC) curves for different parameter sets are shown in FIGURE 17 and FIGURE 18. The x-axis is the false positive rate (FPR), i.e.,  $FPR = T_{D|N}/T_N$ , where  $T_{D|N}$  denotes the time duration of presence detection when the car is empty and  $T_N$  represents the ground-truth duration for the empty car case (Scenario #3 and Scenario #4). On the other hand, the y-axis is the true positive rate (TPR), i.e.,  $TPR = T_{D|P}/T_P$ , where  $T_{D|P}$  denotes the total time of human presence detected by the proposed system when the test subject is in the car and  $T_P$  represents the ground-truth time duration for in-car human presence under Scenario #1 or Scenario #2. FIGURE 17a shows that although a smaller  $\eta_2$  can lead to a better performance in ROC when the false alarm rate is high, it cannot achieve the points for

small false alarm rates. Therefore,  $\eta_2 = 0.6$  is preferred and used in the following comparisons.

FIGURE 17b shows that the performance is similar for different  $\eta_1$  and we choose  $\eta_1 = 0.6$  in the following comparisons. FIGURE 17c compares the performance for different lengths of the moving average window. A longer window can improve the detection performance at a cost of a longer delay of the system. By comparing FIGURE 17 and FIGURE 18, it can be observed that Setting #2 is better for CPD application. This is because the distance between TX and RX is larger and the sensing area is also larger when compared with Setting #1.

### IX. RELATED WORKS AND COMPARISONS

As we have discussed in the previous sections, a car is a special case of indoor environments that delivers large degrees of freedom through plentiful multipaths reflected/scattered by the interior and the metal exterior of the car. Our experimental results showed that the CSI obtained using a single pair of commercial Wi-Fi devices deployed in the car can render meaningful radio analytics. Information about in-car activities, driver state, passenger well-being, and the number of passengers is revealed and thus it enables many cutting-edge IoT applications for the smart car scenario. It can be anticipated that with more bandwidth available in the new generation of wireless communications, one can decipher more multipaths information, and thus achieve better performance.

Besides utilizing CSI directly for wireless sensing [77]–[79], there are other radio analytic techniques in the literature. Traditional wireless passive sensing systems are mainly based on the received signal strength (RSS) [10], [14], [31], [80]. However, because RSS is coarse-grained and can be easily corrupted by multipath effect, RSS-based sensing systems often suffer a limited accuracy in indoor activity detection.

Another category of radio analytic techniques relies on the ToF information embedded in the received signals to track changes of reflected objects for motion detection or vital sign monitoring. As the spatial resolution of the CSI is inversely proportional to the bandwidth, in order to extract the fine-grained ToF information, the ToF-based systems often require either extremely large bandwidths like ultrawide band (UWB) [81]–[83], or specially designed frequency-modulated continuous-wave (FMCW) signals [28], [84]–[87]. Those ToF-based techniques cannot be implemented on off-the-shelf Wi-Fi device and extra calibration is often requested.

Thanks to the advancements in wireless technologies and connective devices, Wi-Fi becomes available in the car, and it delivers enriched multipath information to support IoT applications. The presented wireless AI smart car system show its significant potential and prominent impacts for future smart car applications. The proposed system has no specific requirement for devices and LOS path between the TX and RX and is flexible in device deployment. Moreover, by fully exploiting the magnificent multipath propagation in the car,



the proposed system only requires a single pair of commercial Wi-Fi chipsets and can sense detailed in-car human activity and biological information.

With the development of 5G, millimeter wave (mmWave) has been explored in vital sign monitoring [88]–[90] and other human motion detection applications [91]–[94]. We have conducted experiments for mmWave and in fact the new technology makes sensing much easier because of the high temporal resolution of CSI. However, the cost of mmWave hardware may prevent them from wide deployment, while current 5GHz Wi-Fi can do the sensing tasks sufficiently well. Compared with Wi-Fi signal, there is one more drawback for mmWave sensing that the mmWave cannot penetrate obstructions due to the high carrier frequency and small wave length. Moreover, we also experimented wireless sensing with cellular signals, however, the performance was bad due to the hardware issue and low sampling rate. Sensing with mmWave and 5G cellular signals are beyond the scope of this paper.

### A. EXISTING SMART CAR MONITORING SYSTEMS

Due to the proliferation of automobiles and the advancements in technologies and engineering, there has been a surging demand and interest in IoT applications designed for the smart car, focusing on providing driving assistance and safety enhancement.

Automobile driving is a demanding activity and the state of the driver can bring a significant impact on driving performance. Existing works target more at smart driver monitoring systems that sense and monitor the driver's state and changes in the environment to provide driving assistance, address risk factors associated with driver characteristics, and support driver in maintaining awareness in driving [52]. Smart driver monitoring systems leverage emerging sensor technologies to capture measurements such as driver's facial and body expressions (e.g., percentage of eye closure, frequency of eye blinks and yawning) [60], [95]–[99], driver's interaction with the vehicle (e.g., speed and lane deviation) [100]–[103], and/or driver's physiological signals (e.g., vital sign and brain activity) [49], [50], [63]–[65], [104]–[106]. Although the exact state of a driver may not be directly measurable, systems and algorithms have been designed to infer it from measured data. The information of the driver's facial and body expressions are captured by video cameras or infra-red (IR) cameras which requires a LOS path between the driver and the sensor. Traditional approaches to capture physiological signals of a driver require one to wear sensors during driving. In order to capture one's brain signal, the driver has to put on the EEG sensor over the head. On the other hand, to monitor the driver's vital signs, one is required to either wear ECG sensors or a respiration belt. However, while they are sensing and monitoring driver's state, contact sensors like EEG, ECG and respiration belt can also bring distraction to the driving activity.

Recently, with the development of connective devices, automobile manufacturers have installed Wi-Fi chipsets

and/or Bluetooth into the car. Leveraging the CSI of in-car wireless propagation, Raja *et al.* proposed a Wi-Fi based driver distraction system that infer changes from CSI and then detect unusual head turns and arm movements [66]. However, in that system, the distraction detection was achieved by detecting head and arm movements, both of which often happen during normal driving and may not serve as a reliable feature to evaluate the driver's state.

Compared with the aforementioned methods, the proposed wireless AI smart car system is infrastructure free and non-intrusive, because it relies on the information of multipath propagation between a single pair of commercial Wi-Fi devices without use of cameras or physiological sensors. In addition, as most of the current systems focus only on driver state monitoring, the proposed system in this article succeeds in accomplishing multiple different smart car IoT applications simultaneously, including driver recognition, driver state monitoring, passenger counting, and left child detection in unattended vehicles.

The in-car driver authentication and in-car child presence detection (CPD) are for static cars. For the application of in-car driver authentication, the use case scenario is to identify authorized drivers and then allow the confirmed/recognized driver to start the car. The CPD is designed to detect the presence of a child left in a car after the adult left the car. Hence, when the CPD monitoring is running, the car is most likely to be static. The proposed vital sign monitoring method may not work well when detecting multiple person breathing in a moving car since the breathing detection highly depends on the detection of periodic signals in the CSI time series. However, once the car is static, e.g., waiting before the traffic light, the proposed system can capture the breathing signals and count people.

In addition, the proposed system is immune to outside dynamics and wireless interference. Since the car can be viewed as a closed metal box, most of the multipaths will only propagate in the car and the CSI captured at the Wi-Fi devices will not contain outside information. We conducted experiments in [67] and the results showed that dynamics outside a car, e.g., other cars moving outside the test vehicle, will not affect the in-car sensing. Moreover, even if nearby cars also equip with the proposed Wi-Fi sensing systems, there will not be wireless interference because according to the IEEE802.11 standard, signals transmission on the same Wi-Fi channel follow the collision avoidance protocol.

In the following, we will summarize and compare in detail the existing approaches on smart car monitoring and radio analytics in human recognition, vital sign monitoring, passenger counting, presence detection, and wireless indoor surveillance.

### B. HUMAN RECOGNITION

Human identification can either be done using biometric-based features like the fingerprint, iris, voice, face and etc., or by using non-biometric based features like hand signature, security keys or passwords. Biometric-based approaches have

an inherent advantage over others as they are unique to an individual and cannot be easily forged or forgotten. Although these works can successfully perform human authentication, privacy is compromised. On the other hand, wireless sensing based approaches provide security and privacy at the same time.

Recently, wireless sensing based human identification is receiving an increasing attention. Gait recognition is done by exploiting the variations in CSI patterns and CSI spectrograms [30], [107], [108]. Obtaining gait is not feasible in the proposed smart car system. One of the first work to perform human identification based on wireless sensing used radio biometrics as a feature. Radio biometrics refers to the CSI perturbations as radio signals get reflected and scattered by a human body [44]. This work used time reversal resonating strength (TRRS) to compare different radio biometrics embedded and recorded in the CSI with the assumption that the indoor environment does not change during the period of the experiment. But this assumption is in general false, as can be seen from the change of the in-car environment with time in FIGURE 4.

The NN and SVM techniques were explored for the proposed in-car driver authentication, whose use case is to identify an authorized driver before a car is authorized to start. Hence, given that the environment in a static car should have little vibrations and few interference sources, the current model structure is sufficient for the job. We will explore more complex model structure when we have more data samples and/or different format of samples, e.g., a recurrent neural network (RNN) for a time series of CSI that contains radio biometric information. However, that is out of the scope of this paper.

### C. VITAL SIGN MONITORING

Breathing rate is an important vital sign to monitor human health. Current solutions for breathing monitoring are usually invasive. Wireless sensing techniques capture and record the human breathing signal with EM waves through wireless propagation, and thus supports a contact-free breathing monitoring solution. The existing schemes can be classified into those based on radar [85] and Wi-Fi [39]–[41].

The Universal Software Radio Peripheral (USR) is utilized in [85] as a radar to detect the frequency shift caused by periodic variations of EM waves due to human breath, however, such specialized hardware is highly costly and cannot be widely used. UbiBreath proposed in [39] leverages the RSS of commercial Wi-Fi to extract hidden periodic breathing signal. However, UbiBreath can only detect the breathing signal accurately when the device is close to people's chest. In [40], the fine-grained CSI is used to estimate breathing signal, but the proposed scheme cannot work without knowing the number of people in the coverage area. TR-BREATH in [41] projects CSI into the TRRS and estimates the breathing rate by Root-MUSIC and affinity propagation algorithm. Although TR-BREATH can achieve

a high accuracy, the computational cost is high due to the computational complexity of Root-MUSIC.

Compared with the aforementioned method, the proposed method provides a low-computation cost scheme to estimate the breathing rate by utilizing the off-the-shelf Wi-Fi device. Based on the BPM spectrum obtained by combining the spectrum of CSI on selected links and subcarriers, the proposed scheme is capable of concurrently estimating the breathing rate of multiple people.

The vital sign monitoring can work even when the engine of the car is running but the car is not moving. The detection of vital signs relies on detecting and extracting periodic signals from the time series of captured CSI. As long as the car is static for a while, e.g., stops before a traffic light, the vital signs can be monitored using the proposed method and background noise/interference subtraction for vital signs monitoring in a running is our future work.

### D. PEOPLE COUNTING

Estimating the number of people in a certain area, which is also denoted as crowd counting, is important for many applications. For instance, a smart home can automatically adjust the light and air conditioner based on the number of people. Traditional crowd counting schemes can be classified into two categories: vision-based [109] and RF based [110]–[113].

The performance of the vision-based scheme depends on the setting environment and would degrade severely when the camera is blocked by other objects. Besides, the privacy issue hinders the development of such technology. Radio analytic techniques successfully avoids these problems. Considering the ubiquitous RF devices, there has been considerable interest in RF-based crowd counting. RF-based crowd estimation can be categorized into device-based and device-free methods. As for device-based scheme [110], the system requires users to hold a device, limiting its applicability.

There have been a few works leveraging off-the-shelf Wi-Fi device to do crowd counting [111]–[113]. However, all of these systems are designed based on the assumption that people keep walking in the observation area, which is impractical for the smart car scenario. In our system, we focus on an RF-based device-free method to estimate the number of passengers in the car, which does not require any specific user operations. By identifying and tracking the breathing signal captured by Wi-Fi signals, the proposed iterative DP can estimate the number of passengers in the car with a good accuracy.

### E. CHILD PRESENCE DETECTION

The most prevailing solutions nowadays for CPD are either based on contact sensors, e.g., seat pressure sensor, or based on camera [114] to detect the presence of child in the car. However, both of these two approaches have their own drawbacks. For contact sensor-based approaches, the weight of an infant may be too light to trigger the detection of a seat pressure sensor; for camera-based approaches, the child can

be in the blind zone, e.g., under the rear seats, due to the blockage of the front seats.

Recently, it has been shown in [115] that mmWave sensors can be used to detect the occupancy of each seat in a car, but it requires dedicated hardware and sophisticated signal processing, which limits its deployment in practice. The feasibility of the human motion detection using Wi-Fi devices, which are equipped in many car models, has been proved in [116]–[119]. To the best of our knowledge, we are the first to investigate the use of commercial Wi-Fi devices in the CPD application.

## X. CONCLUSION

Recent developments in wireless technologies and advancements in radio analytics empowers many cutting-edge IoT applications that will dramatically change our lifestyle and assist people in understanding the who, what, when, where, and how of things happening around. Specifically, by leveraging the large degrees of freedom delivered via multipath propagation, one can retrieve the environmental information implanted in the CSI and thus perceive the surrounding world. With larger bandwidth becoming available in the next generation communications, richer information can be revealed by the means of wireless sensing.

As the number of automobiles is proliferating and vehicles are becoming increasingly automated, it is important for the vehicle to be intelligent and provide driving assistance and safety guarantee. The inside of a car can be viewed as a special case of rich scattering indoor environments, where multipath propagation interacts with the driver and the passengers, meanwhile, recording their characteristics. Inspired by the techniques of radio analytics, we proposed the concept of wireless AI for smart cars, introducing smart IoT applications to the car. With the help of a pair of commercial Wi-Fi devices deployed in the car, the proposed wireless AI system can automatically identify the driver, monitor the driver's state, count number of people sitting in the car, and detect the presence of the unattended/left child. Unlike traditional approaches for smart car monitoring, the proposed wireless AI approach utilizes non-intrusive sensing, enjoys low complexity, works well under NLOS, and supports multiple IoT applications simultaneously, thus making it an ideal paradigm for the future smart car monitoring.

## REFERENCES

- [1] B. Wang, Q. Xu, C. Chen, F. Zhang, and K. J. R. Liu, "The promise of radio analytics: A future paradigm of wireless positioning, tracking, and sensing," *IEEE Signal Process. Mag.*, vol. 35, no. 3, pp. 59–80, May 2018.
- [2] J. M. F. Moura and Y. Jin, "Detection by time reversal: Single antenna," *IEEE Trans. Signal Process.*, vol. 55, no. 1, pp. 187–201, Jan. 2007.
- [3] Y. Jin, J. M. F. Moura, Y. Jiang, D. D. Stancil, and A. G. Cepni, "Time reversal detection in clutter: Additional experimental results," *IEEE Trans. Aerosp. Electron. Syst.*, vol. 47, no. 1, pp. 140–154, Jan. 2011.
- [4] Y. Chen, F. Han, Y.-H. Yang, H. Ma, Y. Han, C. Jiang, H.-Q. Lai, D. Claffey, Z. Safar, and K. J. R. Liu, "Time-reversal wireless paradigm for green Internet of Things: An overview," *IEEE Internet Things J.*, vol. 1, no. 1, pp. 81–98, Feb. 2014.
- [5] G. Lerosey, J. de Rosny, A. Tourin, A. Derode, G. Montaldo, and M. Fink, "Time reversal of electromagnetic waves," *Phys. Rev. Lett.*, vol. 92, no. 19, May 2004, Art. no. 193904.
- [6] M. A. A. Al-qaness, F. Li, X. Ma, and G. Liu, "Device-free home intruder detection and alarm system using Wi-Fi channel state information," *Int. J. Future Comput. Commun.*, vol. 5, no. 4, p. 180, 2016.
- [7] Q. Xu, Y. Chen, B. Wang, and K. J. R. Liu, "TRIEDS: Wireless events detection through the wall," *IEEE Internet Things J.*, vol. 4, no. 3, pp. 723–735, Jun. 2017.
- [8] K. Ohara, T. Maekawa, and Y. Matsushita, "Detecting state changes of indoor everyday objects using Wi-Fi channel state information," *ACM Interact., Mobile, Wearable Ubiquitous Technol.*, vol. 1, no. 3, pp. 1–28, Sep. 2017.
- [9] Q. Xu, Z. Safar, Y. Han, B. Wang, and K. J. R. Liu, "Statistical learning over time-reversal space for indoor monitoring system," *IEEE Internet Things J.*, vol. 5, no. 2, pp. 970–983, Apr. 2018.
- [10] Y. Wang, K. Wu, and L. M. Ni, "WiFall: Device-free fall detection by wireless networks," in *Proc. Int. Conf. Comput. Commun.*, Apr. 2014, pp. 271–279.
- [11] Y. Zeng, P. H. Pathak, C. Xu, and P. Mohapatra, "Your AP knows how you move: Fine-grained device motion recognition through WiFi," in *Proc. 1st ACM Workshop Hot Topics in Wireless*, 2014, pp. 49–54.
- [12] Y. Wang, J. Liu, Y. Chen, M. Gruteser, J. Yang, and H. Liu, "E-eyes: Device-free location-oriented activity identification using fine-grained WiFi signatures," in *Proc. 20th ACM Annu. Int. Conf. Mobile Comput. Netw.*, 2014, pp. 617–628.
- [13] W. Wang, A. X. Liu, M. Shahzad, K. Ling, and S. Lu, "Understanding and modeling of WiFi signal based human activity recognition," in *Proc. 21st Annu. Int. Conf. Mobile Comput. Netw. (MobiCom)*, 2015, pp. 65–76.
- [14] Y. Gu, F. Ren, and J. Li, "PAWS: Passive human activity recognition based on WiFi ambient signals," *IEEE Internet Things J.*, vol. 3, no. 5, pp. 796–805, Oct. 2016.
- [15] N. Ghourchian, "Location-based activity recognition with hierarchical Dirichlet process," in *Proc. 25th Int. Joint Conf. Artif. Intell.*, 2016, pp. 3990–3991.
- [16] Y.-X. Zhao, N.-X. Du, Z.-Y. Fang, and H.-Y. Sun, "Design and implementation of frequency domain feature extraction module for human motion recognition," in *Proc. Int. Conf. Wireless Commun., Netw. Appl. (WCNA)*, 2017, pp. 51–56.
- [17] F. Zhang, C. Chen, B. Wang, and K. J. R. Liu, "WiSpeed: A statistical electromagnetic approach for device-free indoor speed estimation," *IEEE Internet Things J.*, vol. 5, no. 3, pp. 2163–2177, Jun. 2018.
- [18] S. S. Souvik, R. R. Choudhury, and S. Nelakuditi, "SpinLoc: Spin once to know your location," in *Proc. 12th Workshop Mobile Comput. Syst. Appl. (HotMobile)*, New York, NY, USA, 2012, pp. 12:1–12:6.
- [19] S. Sen, B. Radunovic, R. R. Choudhury, and T. Minka, "You are facing the Mona Lisa: Spot localization using PHY layer information," in *Proc. 10th Int. Conf. Mobile Syst., Appl., Services (MobiSys)*, 2012, pp. 183–196.
- [20] K. Wu, J. Xiao, Y. Yi, D. Chen, X. Luo, and L. M. Ni, "CSI-based indoor localization," *IEEE Trans. Parallel Distrib. Syst.*, vol. 24, no. 7, pp. 1300–1309, Jul. 2013.
- [21] M. Z. Win, "Multipath-assisted indoor positioning," Ph.D. dissertation, Massachusetts Inst. Technol., Cambridge, MA, USA, 2014.
- [22] M. Kotaru, K. Joshi, D. Bharadia, and S. Katti, "SpotFi: Decimeter level localization using WiFi," in *Proc. ACM SIGCOMM Comput. Commun. Rev.*, vol. 45, no. 4, 2015, pp. 269–282.
- [23] X. Wang, L. Gao, S. Mao, and S. Pandey, "DeepFi: Deep learning for indoor fingerprinting using channel state information," in *Proc. IEEE Wireless Commun. Netw. Conf. (WCNC)*, Mar. 2015, pp. 1666–1671.
- [24] Z.-H. Wu, Y. Han, Y. Chen, and K. J. R. Liu, "A time-reversal paradigm for indoor positioning system," *IEEE Trans. Veh. Technol.*, vol. 64, no. 4, pp. 1331–1339, Apr. 2015.
- [25] K. Lin, M. Chen, J. Deng, M. M. Hassan, and G. Fortino, "Enhanced fingerprinting and trajectory prediction for IoT localization in smart buildings," *IEEE Trans. Autom. Sci. Eng.*, vol. 13, no. 3, pp. 1294–1307, Jul. 2016.
- [26] C. Chen, Y. Chen, Y. Han, H.-Q. Lai, F. Zhang, and K. J. R. Liu, "Achieving centimeter-accuracy indoor localization on wifi platforms: A multi-antenna approach," *IEEE Internet Things J.*, vol. 4, no. 1, pp. 122–134, Feb. 2017.
- [27] C. Chen, Y. Chen, Y. Han, H.-Q. Lai, and K. J. R. Liu, "Achieving centimeter-accuracy indoor localization on wifi platforms: A frequency hopping approach," *IEEE Internet Things J.*, vol. 4, no. 1, pp. 111–121, Feb. 2017.



- [28] F. Adib, C.-Y. Hsu, H. Mao, D. Katabi, and F. Durand, "Capturing the human figure through a wall," *ACM Trans. Graph.*, vol. 34, no. 6, pp. 219:1–219:13, Oct. 2015.
- [29] Y. Li and T. Zhu, "Using Wi-Fi signals to characterize human gait for identification and activity monitoring," in *Proc. IEEE 1st Int. Conf. Connected Health, Appl., Syst. Eng. Technol. (CHASE)*, Jun. 2016, pp. 238–247.
- [30] Y. Zeng, P. H. Pathak, and P. Mohapatra, "WiWho: WiFi-based person identification in smart spaces," in *Proc. 15th ACM/IEEE Int. Conf. Inf. Process. Sensor Netw. (IPSN)*, Apr. 2016, p. 4.
- [31] D. Zhang, J. Ma, Q. Chen, and L. M. Ni, "An RF-based system for tracking transceiver-free objects," in *Proc. 5th Annu. IEEE Int. Conf. Pervasive Comput. Commun. (PerCom)*, Mar. 2007, pp. 135–144.
- [32] F. Adib, Z. Kabelac, and D. Katabi, "Multi-person localization via RF body reflections," in *Proc. 12th USENIX Symp. Netw. Syst. Design Implement.*, May 2015, pp. 279–292.
- [33] Q. Xu, F. Zhang, B. Wang, and K. J. R. Liu, "Time reversal indoor tracking with centimeter accuracy," in *Proc. IEEE Int. Conf. Acoust., Speech Signal Process. (ICASSP)*, Apr. 2018, p. 1.
- [34] F. Zhang, C. Chen, B. Wang, H.-Q. Lai, Y. Han, and K. J. R. Liu, "WiBall: A time-reversal focusing ball method for decimeter-accuracy indoor tracking," *IEEE Internet Things J.*, vol. 5, no. 5, pp. 4031–4041, Oct. 2018.
- [35] Q. Pu, S. Gupta, S. Gollakota, and S. Patel, "Whole-home gesture recognition using wireless signals," in *Proc. 19th Annu. Int. Conf. Mobile Comput. Netw. (MobiCom)*, 2013, pp. 27–38.
- [36] K. Ali, A. X. Liu, W. Wang, and M. Shahzad, "Keystroke recognition using WiFi signals," in *Proc. 21st Annu. Int. Conf. Mobile Comput. Netw. (MobiCom)*, 2015, pp. 90–102.
- [37] S. Tan and J. Yang, "WiFinger: Leveraging commodity WiFi for fine-grained finger gesture recognition," in *Proc. 17th ACM Int. Symp. Mobile Ad Hoc Netw. Comput. (MobiHoc)*, 2016, pp. 201–210.
- [38] R. Ravichandran, E. Saba, K.-Y. Chen, M. Goel, S. Gupta, and S. N. Patel, "WiBreathe: Estimating respiration rate using wireless signals in natural settings in the home," in *Proc. IEEE Int. Conf. Pervasive Comput. Commun. (PerCom)*, Mar. 2015, pp. 131–139.
- [39] H. Abdelnasser, K. A. Harras, and M. Youssef, "UbiBreathe: A ubiquitous non-invasive WiFi-based breathing estimator," in *Proc. 16th Int. Symp. Mobile Ad Hoc Netw. Comput. (MobiHoc)*, New York, NY, USA, 2015, pp. 277–286.
- [40] J. Liu, Y. Wang, Y. Chen, J. Yang, X. Chen, and J. Cheng, "Tracking vital signs during sleep leveraging off-the-shelf WiFi," in *Proc. 16th ACM Int. Symp. Mobile Ad Hoc Netw. Comput. (MobiHoc)*, 2015, pp. 267–276.
- [41] C. Chen, Y. Han, Y. Chen, H.-Q. Lai, F. Zhang, B. Wang, and K. J. R. Liu, "TR-BREATH: Time-reversal breathing rate estimation and detection," *IEEE Trans. Biomed. Eng.*, vol. 65, no. 3, pp. 489–501, Mar. 2018.
- [42] P. Beckmann and A. Spizzichino, *The Scattering of Electromagnetic Waves from Rough Surfaces*. Norwood, MA, USA: Artech House, 1987, p. 511.
- [43] G. Melia, "Electromagnetic absorption by the human body from 1-15 GHz," Ph.D. dissertation, Univ. York, York, U.K., 2013.
- [44] Q. Xu, Y. Chen, B. Wang, and K. J. R. Liu, "Radio biometrics: Human recognition through a wall," *IEEE Trans. Inf. Forensics Security*, vol. 12, no. 5, pp. 1141–1155, May 2017.
- [45] *Number of Vehicles Per Household in the United States From 2006 to 2016*. Accessed: Feb. 1, 2019. [Online]. Available: <https://www.statista.com/statistics/551403/number-of-vehicles-per-household-in-the-united-states/>
- [46] *Number of Passenger Cars and Commercial Vehicles in Use Worldwide From 2006 to 2015 in (1, 000 Units)*. Accessed: Feb. 1, 2019. [Online]. Available: <https://www.statista.com/statistics/281134/number-of-vehicles-in-use-worldwide>
- [47] J. F. Coughlin, B. Reimer, and B. Mehler, "Monitoring, managing, and motivating driver safety and well-being," *IEEE Pervasive Comput.*, vol. 10, no. 3, pp. 14–21, Jul. 2011.
- [48] J. Edwards, "Signal processing: The driving force behind smarter, safer, and more connected vehicles [special reports]," *IEEE Signal Process. Mag.*, vol. 28, no. 5, pp. 8–13, Sep. 2011.
- [49] B.-G. Lee and W.-Y. Chung, "Driver alertness monitoring using fusion of facial features and bio-signals," *IEEE Sensors J.*, vol. 12, no. 7, pp. 2416–2422, Jul. 2012.
- [50] S.-J. Jung, H.-S. Shin, and W.-Y. Chung, "Driver fatigue and drowsiness monitoring system with embedded electrocardiogram sensor on steering wheel," *IET Intell. Transp. Syst.*, vol. 8, no. 1, pp. 43–50, Feb. 2014.
- [51] J. H. L. Hansen, C. Busso, Y. Zheng, and A. Sathyanarayana, "Driver modeling for detection and assessment of driver distraction: Examples from the UTDrive test bed," *IEEE Signal Process. Mag.*, vol. 34, no. 4, pp. 130–142, Jul. 2017.
- [52] A. S. Aghaei, B. Donmez, C. C. Liu, D. He, G. Liu, K. N. Plataniotis, H.-Y.-W. Chen, and Z. Sojoudi, "Smart driver monitoring: When signal processing meets human factors: In the driver's seat," *IEEE Signal Process. Mag.*, vol. 33, no. 6, pp. 35–48, Nov. 2016.
- [53] K. R. Liu and B. Wang, *Wireless AI: Wireless Sensing, Positioning, IoT, and Communications*. Cambridge, U.K.: Cambridge Univ. Press, 2019.
- [54] *Heatstroke Deaths of Children in Vehicles*. Accessed: Feb. 1, 2019. [Online]. Available: <https://www.noheatstroke.org/index.htm>
- [55] Q. Xu, C. Jiang, Y. Han, B. Wang, and K. J. R. Liu, "Waveforming: An overview with beamforming," *IEEE Commun. Surveys Tuts.*, vol. 20, no. 1, pp. 132–149, 1st Quart., 2018.
- [56] J. G. Andrews, S. Buzzi, W. Choi, S. V. Hanly, A. Lozano, A. C. K. Soong, and J. C. Zhang, "What will 5G be?" *IEEE J. Sel. Areas Commun.*, vol. 32, no. 6, pp. 1065–1082, Jun. 2014.
- [57] B. Wang, Y. Wu, F. Han, Y.-H. Yang, and K. J. R. Liu, "Green wireless communications: A time-reversal paradigm," *IEEE J. Sel. Areas Commun.*, vol. 29, no. 8, pp. 1698–1710, Sep. 2011.
- [58] S. Singh, "Critical reasons for crashes investigated in the national motor vehicle crash causation survey," US Dept. Transp., Nat. Highway Traffic Saf. Admin. NHTSA's, Washington, DC, USA, Tech. Rep. DOT HS 812115, 2015.
- [59] Q. Wang, J. Yang, M. Ren, and Y. Zheng, "Driver fatigue detection: A survey," in *Proc. 6th World Congr. Intell. Control Autom.*, 2006, pp. 8587–8591.
- [60] Y. Dong, Z. Hu, K. Uchimura, and N. Murayama, "Driver inattention monitoring system for intelligent vehicles: A review," *IEEE Trans. Intell. Transp. Syst.*, vol. 12, no. 2, pp. 596–614, Jun. 2011.
- [61] E. Wahlstrom, O. Masoud, and N. Papanikolopoulos, "Vision-based methods for driver monitoring," in *Proc. IEEE Int. Conf. Intell. Transp. Syst.*, vol. 2, 2003, pp. 903–908.
- [62] W. Rong-Ben, G. Ke-You, S. Shu-Ming, and C. Jiang-Wei, "A monitoring method of driver fatigue behavior based on machine vision," in *Proc. IEEE IV Intell. Vehicles Symp.*, Jun. 2003, pp. 110–113.
- [63] J. A. Healey and R. W. Picard, "Detecting stress during real-world driving tasks using physiological sensors," *IEEE Trans. Intell. Transp. Syst.*, vol. 6, no. 2, pp. 156–166, Jun. 2005.
- [64] H. B. Lee, J. M. Choi, J. S. Kim, Y. S. Kim, H. J. Baek, M. S. Ryu, R. H. Sohn, and K. S. Park, "Nonintrusive biosignal measurement system in a vehicle," in *Proc. 29th Annu. Int. Conf. IEEE Eng. Med. Biol. Soc.*, Aug. 2007, pp. 2303–2306.
- [65] S. Begum, "Intelligent driver monitoring systems based on physiological sensor signals: A review," in *Proc. 16th Int. IEEE Conf. Intell. Transp. Syst. (ITSC)*, Oct. 2013, pp. 282–289.
- [66] M. Raja, V. Ghaderi, and S. Sigg, "Detecting driver's distracted behaviour from Wi-Fi," in *Proc. IEEE 87th Veh. Technol. Conf. (VTC Spring)*, Jun. 2018, pp. 1–5.
- [67] S. D. Regani, Q. Xu, B. Wang, M. Wu, and K. J. R. Liu, "Driver authentication for smart car using wireless sensing," *IEEE Internet Things J.*, to be published.
- [68] S. Gabriel, R. W. Lau, and C. Gabriel, "The dielectric properties of biological tissues: II. Measurements in the frequency range 10 Hz to 20 GHz," *Phys. Med. Biol.*, vol. 41, no. 11, pp. 2251–2269, Nov. 1996.
- [69] S. Gabriel, R. W. Lau, and C. Gabriel, "The dielectric properties of biological tissues: III. parametric models for the dielectric spectrum of tissues," *Phys. Med. Biol.*, vol. 41, no. 11, pp. 2271–2293, Nov. 1996.
- [70] D. W. Aha, D. Kibler, and M. K. Albert, "Instance-based learning algorithms," *Mach. Learn.*, vol. 6, no. 1, pp. 37–66, Jan. 1991, doi: [10.1007/BF00153759](https://doi.org/10.1007/BF00153759).
- [71] S. Tong and D. Koller, "Support vector machine active learning with applications to text classification," *J. Mach. Learn. Res.*, vol. 2, pp. 45–66, Nov. 2001.
- [72] W. S. Noble, "Support vector machine applications in computational biology," in *Kernel Methods in Computational Biology*, vol. 71. Cambridge, MA, USA: MIT Press, 2004, p. 92.
- [73] L. Wang, *Support Vector Machines: Theory and Applications*. Berlin, Germany: Springer, 2005, vol. 177.
- [74] M. Stone, "Cross-validated choice and assessment of statistical predictions," *J. Roy. Stat. Soc., B, Methodol.*, vol. 36, no. 2, pp. 111–133, Jan. 1974.



- [75] B. Mehler, B. Reimer, J. F. Coughlin, and J. A. Dusek, "Impact of incremental increases in cognitive workload on physiological arousal and performance in young adult drivers," *Transp. Res. Rec., J. Transp. Res. Board*, vol. 2138, no. 1, pp. 6–12, Jan. 2009.
- [76] G. E. Box, G. M. Jenkins, G. C. Reinsel, and G. M. Ljung, *Time Series Analysis: Forecasting and Control, 5th Edition*. Hoboken, NJ, USA: Wiley, 2015.
- [77] Z. Tian, J. Wang, X. Yang, and M. Zhou, "WiCatch: A Wi-Fi based hand gesture recognition system," *IEEE Access*, vol. 6, pp. 16911–16923, 2018.
- [78] Z. Wang, K. Jiang, Y. Hou, Z. Huang, W. Dou, C. Zhang, and Y. Guo, "A survey on CSI-based human behavior recognition in Through-the-Wall scenario," *IEEE Access*, vol. 7, pp. 78772–78793, 2019.
- [79] M. A. A. Al-qaness, M. Abd Elaziz, S. Kim, A. A. Ewees, A. A. Abbasi, Y. A. Alhaj, and A. Hawbani, "Channel state information from pure communication to sense and track human motion: A survey," *Sensors*, vol. 19, no. 15, p. 3329, 2019.
- [80] H. Abdelnasser, M. Youssef, and K. A. Harras, "WiGest: A ubiquitous Wi-Fi-based gesture recognition system," in *Proc. IEEE Conf. Comput. Commun.*, Apr. 2015, pp. 1472–1480.
- [81] G. K. Nanani and K. M. V. V. Prasad, "A study of Wi-Fi based system for moving object detection through the wall," *Int. J. Comput. Appl.*, vol. 79, no. 7, pp. 15–18, 2013.
- [82] Y. Zhu, Y. Zhu, B. Y. Zhao, and H. Zheng, "Reusing 60 GHz radios for mobile radar imaging," in *Proc. 21st Annu. Int. Conf. Mobile Comput. Netw. (MobiCom)*, 2015, pp. 103–116.
- [83] D. Vasisht, S. Kumar, and D. Katabi, "Decimeter-level localization with a single WiFi access point," in *Proc. 13th USENIX Symp. Netw. Syst. Design Implement. (NSDI)*, 2016, pp. 165–178.
- [84] F. Adib, Z. Kabelac, D. Katabi, and R. C. Miller, "3D tracking via body radio reflections," in *Proc. 11th USENIX Conf. Netw. Syst. Design Implement.*, Seattle, WA, USA, Apr. 2014, pp. 317–329.
- [85] F. Adib, H. Mao, Z. Kabelac, D. Katabi, and R. C. Miller, "Smart homes that monitor breathing and heart rate," in *Proc. 33rd Annu. ACM Conf. Hum. Factors Comput. Syst. (CHI)*, 2015, pp. 837–846.
- [86] C.-Y. Hsu, Y. Liu, Z. Kabelac, R. Hristov, D. Katabi, and C. Liu, "Extracting gait velocity and stride length from surrounding radio signals," in *Proc. Conf. Hum. Factors Comput. Syst. (CHI)*, 2017, pp. 2116–2126.
- [87] M. Zhao, S. Yue, D. Katabi, T. S. Jaakkola, and M. T. Bianchi, "Learning sleep stages from radio signals: A conditional adversarial architecture," in *Proc. 34th Int. Conf. Mach. Learn.*, vol. 70, Aug. 2017, pp. 4100–4109.
- [88] S. Bakhtiari, T. W. Elmer, N. M. Cox, N. Gopalsami, A. C. Raptis, S. Liao, I. Mikhelson, and A. V. Sahakian, "Compact millimeter-wave sensor for remote monitoring of vital signs," *IEEE Trans. Instrum. Meas.*, vol. 61, no. 3, pp. 830–841, Mar. 2012.
- [89] Z. Yang, P. H. Pathak, Y. Zeng, X. Liran, and P. Mohapatra, "Monitoring vital signs using millimeter wave," in *Proc. 17th ACM Int. Symp. Mobile Ad Hoc Netw. Comput. (MobiHoc)*, New York, NY, USA, 2016, pp. 211–220, doi: 10.1145/2942358.2942381.
- [90] Z. Yang, P. H. Pathak, Y. Zeng, X. Liran, and P. Mohapatra, "Vital sign and sleep monitoring using millimeter wave," *ACM Trans. Sensor Netw.*, vol. 13, no. 2, pp. 1–32, Apr. 2017, doi: 10.1145/3051124.
- [91] J. Lien, N. Gillian, M. E. Karagozler, P. Amihhood, C. Schwesig, E. Olson, H. Raja, and I. Poupyrev, "Soli: Ubiquitous gesture sensing with millimeter wave radar," *ACM Trans. Graph.*, vol. 35, no. 4, pp. 1–19, Jul. 2016, doi: 10.1145/2897824.2925953.
- [92] Y. Zeng, P. H. Pathak, Z. Yang, and P. Mohapatra, "Poster abstract: Human tracking and activity monitoring using 60 GHz mmWave," in *Proc. 15th ACM/IEEE Int. Conf. Inf. Process. Sensor Netw. (IPSN)*, Apr. 2016, pp. 1–2.
- [93] X. Wang, L. Kong, F. Kong, F. Qiu, M. Xia, S. Arnon, and G. Chen, "Millimeter wave communication: A comprehensive survey," *IEEE Commun. Surveys Tuts.*, vol. 20, no. 3, pp. 1616–1653, 3rd Quart., 2018.
- [94] R. Zhang and S. Cao, "Real-time human motion behavior detection via CNN using mmWave radar," *IEEE Sensors Lett.*, vol. 3, no. 2, pp. 1–4, Feb. 2019.
- [95] D. F. Dinges and R. Grace, "Perclos: A valid psychophysiological measure of alertness as assessed by psychomotor vigilance," U.S. Dept. Transp., Federal Highway Admin., Washington, DC, USA, Tech. Rep. FHWA-MCRT-98-006, 1998.
- [96] Q. Ji, P. Lan, and C. Looney, "A probabilistic framework for modeling and real-time monitoring human fatigue," *IEEE Trans. Syst., Man, Cybern. A, Syst. Humans*, vol. 36, no. 5, pp. 862–875, Sep. 2006.
- [97] I. Park, J.-H. Ahn, and H. Byun, "Efficient measurement of eye blinking under various illumination conditions for drowsiness detection systems," in *Proc. 18th Int. Conf. Pattern Recognit. (ICPR)*, 2006, pp. 383–386.
- [98] M.-H. Sigari, M. Fathy, and M. Soryani, "A driver face monitoring system for fatigue and distraction detection," *Int. J. Veh. Technol.*, vol. 2013, pp. 1–11, 2013, doi: 10.1155/2013/263983.
- [99] R. Oyini Mbouna, S. G. Kong, and M.-G. Chun, "Visual analysis of eye state and head pose for driver alertness monitoring," *IEEE Trans. Intell. Transp. Syst.*, vol. 14, no. 3, pp. 1462–1469, Sep. 2013.
- [100] M. Bayly, K. L. Young, and M. A. Regan, "12 sources of distraction inside the vehicle and their effects on driving performance," in *Driver Distraction: Theory, Effects, and Mitigation*. Boca Raton, FL, USA: CRC Press, 2008, p. 191.
- [101] F. Tango, C. Calefato, L. Minin, and L. Canovi, "Moving attention from the road: A new methodology for the driver distraction evaluation using machine learning approaches," in *Proc. 2nd Conf. Hum. Syst. Interact.*, May 2009, pp. 596–599.
- [102] C. C. Liu, S. G. Hosking, and M. G. Lenné, "Predicting driver drowsiness using vehicle measures: Recent insights and future challenges," *J. Saf. Res.*, vol. 40, no. 4, pp. 239–245, Aug. 2009.
- [103] A. Sahayadhas, K. Sundaraj, and M. Murugappan, "Detecting driver drowsiness based on sensors: A review," *Sensors*, vol. 12, no. 12, pp. 16937–16953, 2012.
- [104] M. Walter, B. Eilebrecht, T. Wartzek, and S. Leonhardt, "The smart car seat: Personalized monitoring of vital signs in automotive applications," *Pers. Ubiquitous Comput.*, vol. 15, no. 7, pp. 707–715, Oct. 2011, doi: 10.1007/s00779-010-0350-4.
- [105] C. Zhao, M. Zhao, J. Liu, and C. Zheng, "Electroencephalogram and electrocardiograph assessment of mental fatigue in a driving simulator," *Accident Anal. Prevention*, vol. 45, pp. 83–90, Mar. 2012.
- [106] G. Borghini, L. Astolfi, G. Vecchiato, D. Mattia, and F. Babiloni, "Measuring neurophysiological signals in aircraft pilots and car drivers for the assessment of mental workload, fatigue and drowsiness," *Neurosci. Biobehavioral Rev.*, vol. 44, pp. 58–75, Jul. 2014.
- [107] W. Wang, A. X. Liu, and M. Shahzad, "Gait recognition using WiFi signals," in *Proc. ACM Int. Joint Conf. Pervasive Ubiquitous Comput. (UbiComp)*, 2016, pp. 363–373.
- [108] J. Zhang, B. Wei, W. Hu, and S. S. Kanhere, "WiFi-ID: Human identification using WiFi signal," in *Proc. Int. Conf. Distrib. Comput. Sensor Syst. (DCOSS)*, May 2016, pp. 75–82.
- [109] Y. Zhang, D. Zhou, S. Chen, S. Gao, and Y. Ma, "Single-image crowd counting via multi-column convolutional neural network," in *Proc. IEEE Conf. Comput. Vis. Pattern Recognit. (CVPR)*, Jun. 2016, pp. 589–597.
- [110] H. Zou, H. Jiang, Y. Luo, J. Zhu, X. Lu, and L. Xie, "BlueDetect: An iBeacon-enabled scheme for accurate and energy-efficient indoor-outdoor detection and seamless location-based service," *Sensors*, vol. 16, no. 2, p. 26, 2016.
- [111] S. Depatla and Y. Mostofi, "Crowd counting through walls using WiFi," in *Proc. IEEE Int. Conf. Pervasive Comput. Commun. (PerCom)*, Mar. 2018, pp. 1–10.
- [112] H. Zou, Y. Zhou, J. Yang, W. Gu, L. Xie, and C. Spanos, "FreeCount: Device-free crowd counting with commodity WiFi," in *Proc. IEEE Global Commun. Conf. (GLOBECOM)*, Dec. 2017, pp. 1–6.
- [113] S. Di Domenico, M. De Sanctis, E. Cianca, and G. Bianchi, "A trained-once crowd counting method using differential wifi channel state information," in *Proc. 3rd Int. Workshop Phys. Anal. (WPA)*, New York, NY, USA, 2016, pp. 37–42, doi:
- [114] A. Makrushin, M. Langnickel, M. Schott, C. Vielhauer, J. Dittmann, and K. Seifert, "Car-seat occupancy detection using a monocular 360° NIR camera and advanced template matching," in *Proc. 16th Int. Conf. Digit. Signal Process.*, Jul. 2009, pp. 1–6.
- [115] *Vehicle Occupant Detection Using mmWave Sensors*. Accessed: Mar. 6, 2019. [Online]. Available: <https://training.ti.com/vehicle-occupant-detection-using-mmwave-sensors>
- [116] C. Wu, Z. Yang, Z. Zhou, X. Liu, Y. Liu, and J. Cao, "Non-invasive detection of moving and stationary human with WiFi," *IEEE J. Sel. Areas Commun.*, vol. 33, no. 11, pp. 2329–2342, Nov. 2015.
- [117] K. Qian, C. Wu, Z. Yang, Y. Liu, and Z. Zhou, "PADS: Passive detection of moving targets with dynamic speed using PHY layer information," in *Proc. 20th IEEE Int. Conf. Parallel Distrib. Syst. (ICPADS)*, Dec. 2014.
- [118] H. Zou, Y. Zhou, J. Yang, W. Gu, L. Xie, and C. Spanos, "FreeDetector: Device-free occupancy detection with commodity WiFi," in *Proc. IEEE Int. Conf. Sens., Commun. Netw. (SECON Workshops)*, Jun. 2017, pp. 1–5.

- [119] D. Wu, D. Zhang, C. Xu, H. Wang, and X. Li, "Device-free WiFi human sensing: From pattern-based to model-based approaches," *IEEE Commun. Mag.*, vol. 55, no. 10, pp. 91–97, Oct. 2017.



**QINYI XU** received the B.S. degree (Hons.) in information engineering from Southeast University, China, in July 2013, and the M.S. and Ph.D. degrees in electrical and computer engineering from the University of Maryland at College Park, College Park, MA, USA, in 2016 and 2018, respectively.

She was an Exchange Student at the KTH-Royal Institute of Technology, Stockholm, Sweden, from August 2012 to January 2013, with the National Sponsorship of China. Since July 2018, she has been with Origin Wireless Inc., where she was a Principal Scientist. She was also affiliated with the Department of Electrical and Computer Engineering, University of Maryland at College Park. Her research interests include signal processing, machine learning, wireless sensing, and wireless communications. She was a recipient of the Clark School Distinguished Graduate Fellowships from the University of Maryland at College Park, and the Graduate with Honor Award from Southeast University, in 2013.



**BEIBEI WANG** (Senior Member, IEEE) received the B.S. degree (Hons.) in electrical engineering from the University of Science and Technology of China, Hefei, in 2004, and the Ph.D. degree in electrical engineering from the University of Maryland at College Park, College Park, MA, USA, in 2009. She was with the University of Maryland at College Park as a Research Associate, from 2009 to 2010, and with Qualcomm Research and Development, from 2010 to 2014. Since 2015,

she has been with Origin Wireless Inc., where she is currently the Vice President of Research. She is also affiliated with the University of Maryland at College Park. Her research interests include the Internet of Things, mobile computing, wireless sensing and positioning, and communications and networking. She received the Graduate School Fellowship, the Future Faculty Fellowship, the Dean's Doctoral Research Award from the University of Maryland at College Park, and the Overview Paper Award from the IEEE Signal Processing Society, in 2015. She is a coauthor of the *Cognitive Radio Networking and Security: A Game-Theoretic View* (Cambridge University Press, 2010) and the *Wireless AI: Wireless Sensing, Positioning, IoT, and Communications* (Cambridge University Press, 2019).



**FENG ZHANG** (Member, IEEE) received the B.S. and M.S. degrees from the Department of Electronic Engineering and Information Science, University of Science and Technology of China, Hefei, in 2011 and 2014, respectively, and the Ph.D. degree from the Department of Electrical and Computer Engineering, University of Maryland at College Park, College Park, MA, USA, in December 2018. He is currently the Chief Scientist of Origin Wireless, Inc. His research interests

include wireless sensing, statistical signal processing, and wireless indoor localization. He was a recipient of the Distinguished TA Award from the University of Maryland at College Park and the State Scholarship from the University of Science and Technology of China.



**DEEPIKA SAI REGANI** received the B.Tech. degree in electrical engineering from IIT Madras, India, in 2015, and the M.S. degree from the Department of Electrical and Computer Engineering, University of Maryland at College Park, College Park, MA, USA, in 2017, where she is currently pursuing the Ph.D. degree with the Signal and Information Group. Her research interests include wireless sensing, adaptive signal processing, human radio biometrics, and machine learning.



**FENGYU WANG** received the B.S. and M.S. degrees from the School of Information and Communication Engineering, Beijing University of Posts and Telecommunications, Beijing, China, in 2014 and 2017, respectively. She is currently pursuing the Ph.D. degree with the Department of Electrical and Computer Engineering, University of Maryland at College Park. Her current research interests include wireless sensing and statistical signal processing.



**K. J. RAY LIU** (Fellow, IEEE) is a Distinguished University Professor and a Distinguished Scholar-Teacher with the University of Maryland at College Park, College Park, MA, USA, where he is also a Christine Kim Eminent Professor of information technology. He leads the Maryland Signals and Information Group conducting research encompassing broad areas of information and communications technology, with recent focus on wireless AI for indoor tracking and wireless sensing.

Dr. Liu is a Fellow of the AAAS and National Academy of Inventors. He was a recipient of the 2016 IEEE Leon Kirchmayer Award on graduate teaching and mentoring, the IEEE Signal Processing Society 2014 Society Award, the IEEE Signal Processing Society 2009 Technical Achievement Award, and over a dozen of best paper awards. He is recognized by Web of Science as a Highly Cited Researcher. As the Founder of Origin Wireless, his invention won the 2017 CEATEC Grand Prix Award and the CES 2020 Innovation Award. He was the IEEE Vice President, Technical Activities, and a member of the IEEE Board of Director as Division IX Director. He has served as the President of the IEEE Signal Processing Society, where he was the Vice President–Publications and Board of Governor. He has also served as the Editor-in-Chief for the *IEEE Signal Processing Magazine*. He also received teaching and research recognitions from the University of Maryland at College Park, including the University-Level Invention of the Year Award; and the College-Level Poole and Kent Senior Faculty Teaching Award, the Outstanding Faculty Research Award, and the Outstanding Faculty Service Award, all from A. James Clark School of Engineering.

...